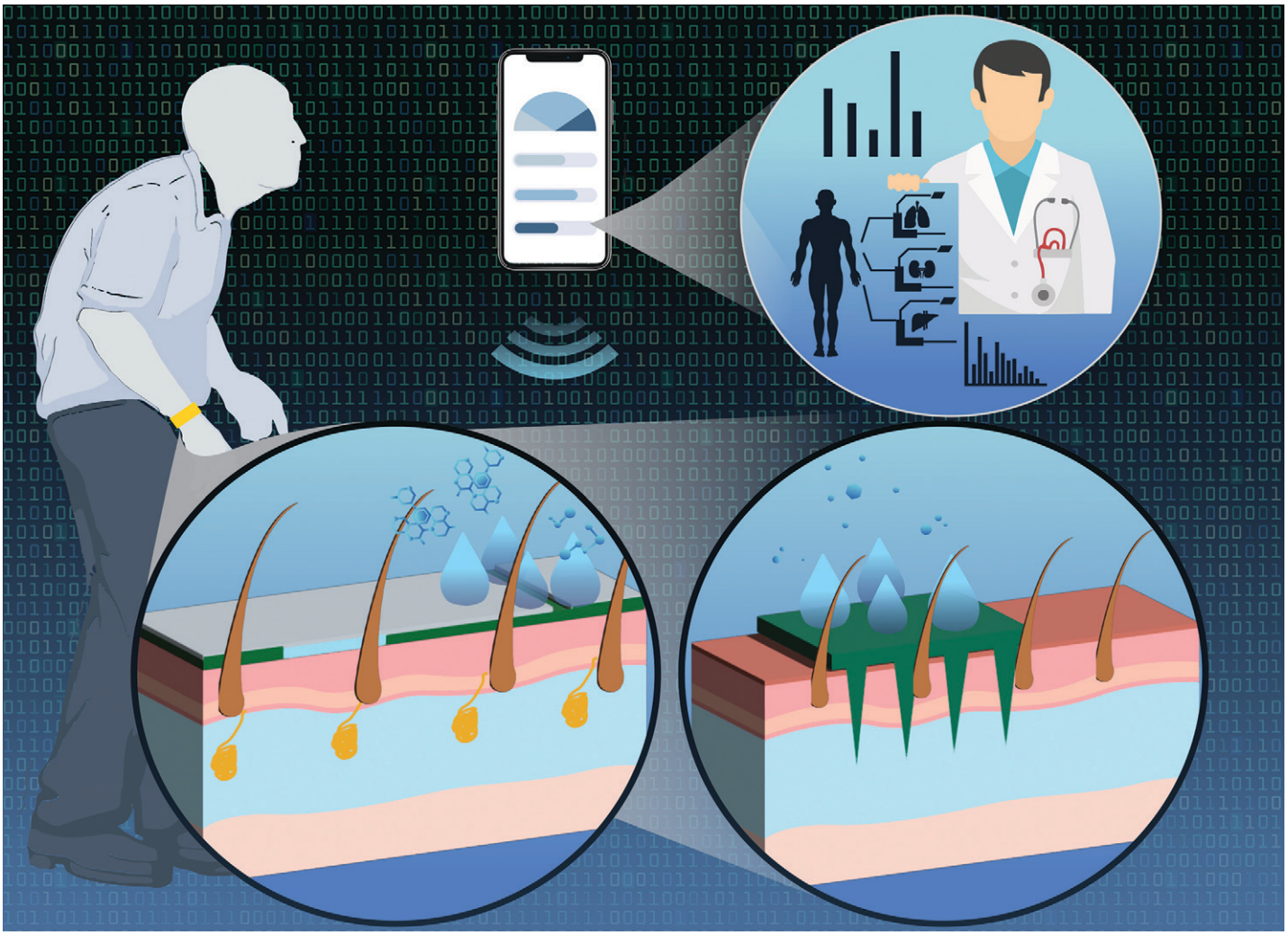

Showcasing research from Professor Hnin Y. Y. NYEIN's laboratory, Department of Chemical and Biological Engineering, the Hong Kong University of Science and Technology, Hong Kong SAR, China.

Dermal-fluid-enabled detection platforms for non-invasive ambulatory monitoring

In this critical review, Hnin Y.Y. Nyein et al. provides detailed analysis and in-depth understanding of the partitioning of critical biomarkers in sweat and interstitial fluid and delineate challenges and opportunities of disposable and wearable technologies for detecting critical biomarkers in dermal fluids (e.g., sweats and interstitial fluids) to achieve non-invasive ambulatory monitoring.

As featured in:

See Hnin Yin Yin Nyein *et al.*, *Sens. Diagn.*, 2023, **2**, 1335.

ROYAL SOCIETY OF CHEMISTRY

rsc.li/sensors

Registered charity number: 207890

Sensors & Diagnostics

CRITICAL REVIEW

View Article Online
View Journal | View Issue

Cite this: *Sens. Diagn.*, 2023, **2**, 1335

Dermal-fluid-enabled detection platforms for non-invasive ambulatory monitoring

Asmita Veronica, Yanan Li, Yue Li, I-Ming Hsing and Hnin Yin Yin Nyein *

The recent COVID-19 pandemic has reminded the healthcare community that realizing remote and ambulatory monitoring while providing clinically relevant health data is critically important. The ability to detect important analytes in easily accessible dermal fluids such as sweat and interstitial fluid (ISF) using disposable and wearable technologies in decentralized settings would be a critical step forward to realize ambulatory care. In this review, we will first provide a detailed description and analysis of the partitioning of major biomarkers of interest in sweat and ISF, followed by in-depth analysis of the clinical relevance of these biomarkers in dermal fluids through providing insightful understanding of their partitioning mechanisms based on literature findings. Using chronic diseases in the aged population and drug monitoring as exemplary cases, we will delineate the development and challenges of sample collection and extraction of dermal fluids and the corresponding state-of-the-art wearable sensors and diagnostics that may hold promise to be implemented in the practical setting of ambulatory monitoring. We believe this in-depth review will be of significant interest to the community as it provides a comprehensive and holistic review and offers a promising outlook on how ambulatory monitoring could be achieved by wearable sensors utilizing non-invasive dermal fluids.

Received 30th June 2023,
Accepted 13th August 2023

DOI: 10.1039/d3sd00165b

rsc.li/sensors

1. Introduction

Ambulatory monitoring is growing in popularity for long-term continuous monitoring and diagnosis in healthcare. Recent developments in remote and mobile healthcare monitoring have enabled economical and practical solutions, which facilitate a new paradigm in healthcare by gathering long-term physiological health data to achieve accurate clinical diagnosis.[1] Most importantly, they allow vulnerable individuals, especially the elderly, to monitor serious health issues at home, reducing the burden associated with hospitalization costs.[2] Ambulatory monitoring offers direct access to information about patients' health status, which can help treat or slow the progression of certain disorders. Also, it can be utilized as a preventive strategy to support a healthy lifestyle.[3,4]

With an increasingly aging population, chronic diseases, such as cardiovascular diseases, diabetes, chronic kidney disease (CKD), *etc.*, are becoming more prevalent worldwide. Chronic diseases cause 41 million deaths globally each year equivalent to 74% of all fatalities, according to the World

Department of Chemical and Biological Engineering, The Hong Kong University of Science and Technology, Clear Water Bay, Hong Kong SAR, China. E-mail: hnyein@ust.hk

Asmita Veronica

Ms. Asmita is currently pursuing her PhD in Bioengineering at HKUST. She received her MSc in Mechanical Engineering with specialization in Materials Technology from HKUST in 2017. She obtained her B. Tech. degree in Metallurgical and Materials Engineering from VNIT, Nagpur, India, in 2015. Her research interests include nanocomposites, biomaterials and wearable bioelectronics.

Yanan Li

Ms. Yanan Li is currently a PhD student in the Department of Chemical and Biological Engineering at The Hong Kong University of Science and Technology (HKUST). She obtained her Master's degree from the University of Science and Technology of China (USTC) in 2022. Her research interests lie in the area of nucleic acid detection and point-of-care testing (POCT).

Health Organization.[5] Unhealthy lifestyle choices contribute to their development and impact every age group, especially the elderly.[6] As healthcare systems around the world have generally focused on acute episodic treatment rather than providing comprehensive care for long-term conditions, addressing chronic disease is still a significant challenge.[7] Moreover, regular visits to clinics and hospitals are impractical and inadequate for the early detection of chronic diseases given their nature and severity, which, if mistreated, can result in fatal complications.[8] Therefore, ambulatory care based on continuous monitoring and diagnostic systems is essential for disease management.

In addition to the clinical examination, laboratory tests of biomarkers are required to make an appropriate diagnosis of medical conditions. Although laboratory-based biomarker detection offers unique parameters, these are not feasible for continuous ambulatory care.[9] The most utilized biomarker sources for testing are blood and urine, which are simple to collect for laboratory analysis and can provide a snapshot of systemic biomarker changes.[10] The gold standard for diagnostics is monitoring biomarkers in blood, but the requirement for qualified healthcare workers to draw venous blood or the patient's anxiety during finger-prick blood sampling makes it unsuitable and invasive. Biofluids such as urine, tears, saliva, sweat, and interstitial fluid (ISF) are less invasive alternatives.[11] Tears do not offer a significant advantage over other biofluids in terms of accessibility for one-time use or continuous monitoring. On the other hand, urine detection is often exclusively employed for single-time, point-of-care (PoC) diagnostics of small molecules because of its varying dilution, low protein content, and irregular synthesis.[12,13] Similarly, saliva is easily accessible for home collection but has been mainly explored for one-time rapid testing. However, the diurnal heterogeneity associated with the composition of the saliva can lead to sample preparation issues and erroneous result interpretation. Also, the low level of biomarkers in saliva as compared to serum and the presence of mucin and proteolytic enzymes make the detection and quantification challenging.[14] In terms of minimally invasive continuous biosensing, sweat and ISF are the leading alternatives to achieve chronic disease management and therapeutic drug monitoring.

Unlike other biofluids, sweat provides plentiful biological information that can be retrieved quickly, non-invasively, on-demand, and continuously.[23] These benefits have fueled enormous attempts to create epidermal sweat sensors to monitor metabolites and electrolytes.[24–27] It has been proposed that analytes in sweat passively or actively move from adjacent blood or ISF at concentrations ranging from mM (*e.g.* urea) to μM (*e.g.* glucose) to nM or pM traces (*e.g.* proteins).[28] However, several limitations in terms of dilution, contamination, and secretion rates still hinder the successful implementation of ambulatory sweat monitoring systems. Moreover, significant improvements

Li Yue

Dr. Li Yue acquired her PhD in the Chemical and Biological Engineering Department at HKUST (2022). She obtained her Master's and Bachelor's degrees in Northeastern University, China. Her research interests include biosensing technologies and soft electronic fabrication for applications in medical practice.

I-Ming Hsing

Dr. I-Ming Hsing is a Professor in the Department of Chemical and Biological Engineering at the Hong Kong University of Science and Technology (HKUST). Dr. Hsing's research interests lie in the interface of molecular biology, reaction engineering, micro/nanofabrication and electrochemistry. Utilizing chemical engineering and molecular engineering principles, his group is interested in nucleic acid engineering and DNA self-assembly for analyte sensing and diagnostic applications for point-of-care testing. His group is also interested in developing organic electrochemical transistors and flexible green bioelectronics and materials for non-invasive and wearable sensing/monitoring biomedical applications.

Hnin Y. Y. Nyein

Dr. Hnin Y. Y. Nyein has been an Assistant Professor in the Department of Chemical and Biological Engineering at the HKUST since 2022. Prior to joining HKUST, she received her PhD from UC Berkeley in 2020 and did postdoc training at Stanford. As a leading author, she has published several pioneer works on wearable sensing technology in major journals including Nature, Nature Communications, Advanced Materials, and ACS Sensors. She was recognized as an innovator in TR35 Asia Pacific 2021 awarded by MIT Technology Review.

in sweat collection and transport are also needed.[29,30] In recent years, researchers have directed their efforts into investigating ISF due to the sample variability induced by the dilution of biomarkers in sweat. Importantly, ISF exhibits little dilution effects for most analytes in terms of molecular weight cutoff and their concentrations are reflective of plasma or serum concentrations.[31,32] Thus, it is a prime candidate for dermal fluid-based ambulatory monitoring. Moreover, technological advancements in ISF have attained commercial maturity for continuous glucose monitoring (CGM) in diabetic patients using an indwelling sensor, which has been widely accepted and growing tremendously due to its high accuracy and low cost.[33] Although, this is an alternative to finger-pricking blood sampling, the invasive nature of this technology does not improve patient compliance. Facile and less invasive ISF sampling techniques employing micro-needle arrays have been attracting interest among researchers in this domain.[10,34]

This review emphasizes the potential of sweat and ISF enabled sensing platforms to complement conventional invasive blood tests to facilitate disease management in ambulatory settings (Fig. 1). We discuss the probable partitioning mechanisms of relevant biomarkers in both the dermal fluids and how they correlate with blood. We also shed light on the existing sweat and ISF sampling technologies and their suitability for long-term monitoring. In addition, a detailed account on the recent developments in sweat and ISF based biosensors and their clinical significance for chronic disease (diabetes and CKD), chronic inflammation and therapeutic drug monitoring is presented. Briefly, the review also provides insights on the current

Fig. 1 Schematic depicting wearable dermal fluid-enabled biomarker detection for remote and non-invasive chronic disease, chronic inflammation, and therapeutic drug monitoring in ambulatory settings (top). The bottom illustration shows recently developed sweat and ISF biosensors for non-invasive analyte monitoring. Reprinted with permission from Lee *et al.*[15] Copyright© 2017 AAAS. Reprinted with permission from Nyein *et al.*[16] Copyright© 2021 Springer Nature. Reprinted with permission from Nyein *et al.*[17] Copyright© 2019 AAAS. Reprinted with permission from He *et al.*[18] Copyright© 2022 Springer Nature. Reprinted with permission from Cheng *et al.*[19] Copyright© 2022 Elsevier. Reprinted with permission from Goud *et al.*[20] Copyright© 2019 American Chemical Society. Reprinted with permission from Sang *et al.*[21] Copyright© 2023 AAAS. Reprinted with permission from Xu *et al.*[22] Copyright© 2023 Wiley-VCH GmbH.

challenges and the future directions in this emerging area of non-invasive detection.

2. Relevance of sweat and ISF for ambulatory monitoring

The analysis of sweat and ISF for ambulatory care is currently underexploited. Understanding of their physiological composition, analyte partitioning pathways, and sampling techniques is essential for drawing accurate correlations between these biofluids and blood, which can accelerate technological advancements in sweat- or ISF-based biosensors. In this section, we will mainly discuss the partitioning mechanisms as depicted in Fig. 2 and correlations for biomarkers in sweat and ISF relevant to chronic diseases, inflammation, and therapeutic drug management for ambulatory care. Table 1 summarizes the concentrations of relevant biomarkers or drugs in sweat, ISF, and blood, molecular size, and corresponding health conditions.

Sweat

Sweat, the most accessible biofluid, plays a vital role in the body through thermoregulation, skin homeostasis, immunity support, moisturization, and pH balance.[35,36] It is produced by eccrine and apocrine sweat glands within the skin. Eccrine sweat is considered the most meaningful and abundant source of analytes, thus ideal for non-invasive sampling and continuous monitoring.[23,37] The eccrine sweat gland primarily consists of a secretory coil at the base for isotonic secretion which straightens into a sweat duct responsible for salt reabsorption ultimately causing the secretion of hypotonic aqueous fluid. Sweat is stimulated either *via* cholinergic or adrenergic nerve fibers in response to thermoregulation and "flight or fight", respectively.[38,39] Acetylcholine, the main neurotransmitter of the eccrine gland, is activated during stimulation, leading to active secretion of chloride which leads to an electrochemical gradient that facilitates the flow of positive sodium ions paracellularly.[35] These ions are actively exchanged between blood and the secretory coil resulting in a buildup of electrolytes in the lumen, which creates a negative osmotic pressure that causes a large influx of water into the sweat gland transcellularly *via* aquaporin and paracellularly *via* ISF.[12,23,28,38,39] At this stage, the aqueous fluid in the coil is isotonic to the cytosol, ISF, and blood. The fluid is then driven up into the sweat duct due to advective flow and the ions are reabsorbed through the ion channels in the duct walls. A hypotonic sweat solution is produced and released onto the skin surface. The neutral pH of the sweat solution in the coil decreases as it moves up the sweat duct; thus final sweat is slightly acidic. The pH of the sweat is dependent on the sweat generation rate and can influence the partitioning of biomolecules.[12,23,28,40,41]

Sweat is a rich biofluid that contains various biomarkers such as electrolytes, metabolites, cytokines, proteins, peptides, and hormones. Hence, the evaluation of these biomarkers' concentrations and flux can provide essential health information.[36,40] The concentration of biomarkers in passive sweat is 10- to 1000-fold lower compared to ISF and blood. However, different analytes can have varying blood-to-sweat correlations as the partitioning depends on their size and charge, sweat rate, and pH.[28] Small uncharged molecules partition transcellularly *via* diffusion through the plasma membrane of the capillary endothelial cells, while paracellular partitioning is characteristic of large hydrophilic molecules *via* diffusion and advective flow through the intercellular space between adjacent cells.[12,23]

Partitioning of relevant biomarkers in sweat. Eccrine sweat is slightly acidic in nature with an average pH of 6.3

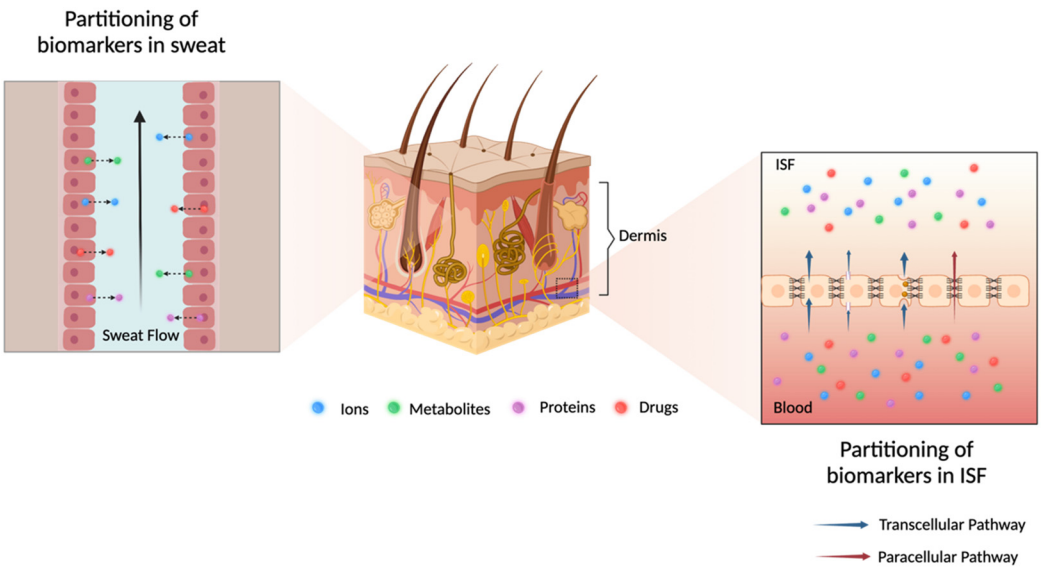

Fig. 2 Illustration of possible partitioning pathways of analytes of interest into dermal fluids sweat (left zoom) and ISF (right zoom).

Table 1 Relevant biomarkers of interest in blood, ISF, and sweat for ambulatory monitoring. [O: oral administration; IV: intravenous administration. C_{max}: maximum concentration]

	Analytes	Blood (μM)	ISF (μM)	Sweat (μM)	Related health condition	Molecular weight (Da)	Ref.
Metabolites	Glucose	$3.6–6.0 \times 10^3$	$0.8–6.0 \times 10^3$	6–300	Diabetes	180	89 and 90
	Urea	$3.0–7.5 \times 10^3$	Similar to plasma	$0.5–2.4 \times 10^4$	Kidney diseases	60	56 and 58
	Creatinine	65–140	18–75	2–18	Kidney diseases	116	31 and 89
	Uric acid	120–450	50–250	18–36	Gout, kidney diseases	168	35 and 56
	β-Hydroxybutyrate	100–600	Similar to plasma	28.9 ± 9.2	Diabetic ketoacidosis	104	91 and 92
Electrolytes	K^+	$3.5–5.5 \times 10^3$	Similar to plasma	$2–10 \times 10^3$	Hydration, kidney diseases	39	35
	NH^{4+}	$0.1–4 \times 10^2$	—	$0.5–8 \times 10^3$	Kidney diseases	18	23
Protein	Tumor necrosis factor-alpha (TNF-α)	$3.4–8.4 \times 10^{-7}$	80% of plasma	$5.4–12.2 \times 10^{-7}$	Inflammation	17.3 k	63 and 93
	Interleukin-1beta (IL-1β)	$1.6–5.3 \times 10^{-7}$		$2.2–5.9 \times 10^{-7}$	Inflammation	31 k	63 and 93
	Interleukin-6 (IL-6)	$2.4–5.6 \times 10^{-7}$		$3.7–6.9 \times 10^{-7}$	Inflammation	21 k	23 and 63
	Interleukin-8 (IL-8)	$1.5–6.5 \times 10^{-7}$		$1.8–7.2 \times 10^{-7}$	Inflammation	8452	23 and 63
	Cystatin C	0.055 ± 0.22	0.254	—	Kidney diseases	13 k	94
Drugs	Levodopa	0.5–15 O (150–550 mg per day)	Similar to plasma	0.1–2.5 O (100–500 mg per day)	Parkinson's disease	197	95
	Acetaminophen	66–132.3 O/IV (1 g per dose)	—	<50	Fever, pain	151	95 and 96
	Penicillin-type	C_{max} 140.5–1342.9 IV (4 g per dose)	C_{max} 32.1–417.3 IV (4 g per dose)	—	Antibiotics for bacterial infection		95
	Vancomycin	13.8–27.6 IV (2 g per day)	C_{max} 22.1 ± 1.8 IV (5–20 mg kg^{-1})	—		1449	95

and is mainly composed of 99% water.[38,42] Potassium (K^+) and ammonium (NH_4^+) ions are key electrolytes for chronic disease monitoring. K^+, known to regulate many vital physiological processes, is present in sweat in the mM range. In a normal kidney, K^+ homeostasis can be maintained irrespective of dietary intake. However, in the case of CKD patients, a diet with high potassium content can lead to further complications and even death.[43] Thus, monitoring K^+ can help predict and prevent potassium disorders in CKD patients. A few studies have suggested that K^+ concentration in sweat is proportional to blood K^+ and independent of sweat rate. However, the exact partitioning pathway of K^+ in sweat is not fully understood yet. K^+ in the secretory coil is isotonic with blood, whereas the sweat released from the sweat duct has a higher concentration of K^+ possibly due to the reabsorption of Na^+.[44] The changes in blood K^+ concentration are insignificant; hence it is difficult to establish a statistically meaningful sweat-to-blood correlation for K^+. Ammonium (NH_4^+) is another electrolyte vital for kidney functioning and infection monitoring.[45,46] Urea build-up during kidney damage can lead to slow processing of ammonia (NH_3), leading to elevated NH_3 concentration in the body. The main source of NH_3 in sweat is blood due to metabolic protein degradation.[47,48] Being a small and uncharged polar molecule, NH_3 partitions into the sweat *via* passive diffusion, where most of the molecules undergo protonation to NH_4^+ due to the pH gradient between the blood and sweat. Low and high sweat generation rates lead to sweat pH 5–7, thereby causing ionization of NH_3. Moreover, the electrical charge on NH_4^+ leads to restricted mobility and causes ion trapping in the lumen, which explains the higher concentration of NH_4^+ in sweat relative to plasma. Ion trapping phenomenon *via* protonation or deprotonation can occur for most of the weak bases or weak acids. Therefore, the design of sensors for these analytes should consider their dependence on pH.[23,49]

Glucose, β-hydroxybutyrate (HB), urea, uric acid (UA), and creatinine are among the relevant metabolites in sweat for ambulatory monitoring. Glucose is monitored in blood samples for diagnosis of prediabetic and diabetic conditions.[50,51] Blood glucose can be correlated to sweat glucose, but the reliability of this correlation is questionable.[17,52] The details of this blood-to-sweat glucose correlation will be discussed in section 3. The partitioning mechanism of glucose in sweat is reported to be paracellular. Although this pathway is dimensionally large, the tight junction selectivity, as a result of plentiful proteins, obstructs the passage of glucose. Moreover, the large size and polarity also further limit mobility leading to filtering and dilution of glucose in sweat which is further influenced by the fluctuating sweat rate.[12,23] Sweat glucose is more diluted during profuse sweating (9 nL min^{-1} per gland) than in passive sweating (1 nL min^{-1} per gland). Nevertheless, sweat glucose is considered an important analyte as it can provide essential information regarding the sweat generation rate and secretion pathways.[53] HB is a ketone body produced in the liver considered a potential indicator of diabetic ketoacidosis, one of the leading causes of mortality in diabetic patients. Although the data correlating sweat-to-blood HB levels are insufficient, a recent study displayed

correlation between sweat HB and blood HB without any significant time delay.[54] Further efforts are required to validate this correlation as well as the clinical relevance of evaluating HB levels in sweat. Urea, a small polar molecule, is widely used to assess kidney function.[55] An early investigation suggests that urea passively diffuses into sweat *via* the paracellular route due to its high diffusivity through cell membranes, with sweat containing higher concentrations compared to blood.[56] Despite high urea levels in sweat relative to serum, no correlation was established between urea levels in these fluids, which suggests that sweat glands may act as an alternative route for waste excretion especially when the kidney function is impaired and the patients are profusely sweating.[57,58] Thus, multiple urea pathways and sweat rate collectively contribute to the sweat urea levels and further clinical studies are needed to understand these behaviors. UA and creatinine are also essential for examining renal function.[56] Both analytes are large, hence are found in lower concentrations (μM range) as compared to blood. UA and creatinine levels in sweat are low to properly understand their partitioning mechanisms.[23,49,58] It was recently found that the sweat UA level was higher in gout patients than in healthy controls, with a similar relationship also observed in serum.[59] Similar to urea, creatinine is present in physiologically relevant ranges in sweat, making it a potential biomarker for CKD monitoring.[60]

Cytokines are proteins that play an important role in protecting the body against viral or bacterial infections. Tumor necrosis factor-alpha (TNF-α), interleukin-6 (IL-6), interleukin-10 (IL-10), interleukin-8 (IL-8) and interleukin-1beta (IL-1β) are important inflammatory biomarkers for chronic inflammation.[61] The partitioning mechanism has not been fully studied but it has been hypothesized that cytokines are released from the intravascular membrane during inflammation and transported into the dermal interstitium despite the filtering effect of tight junctions mainly due to the remodelling.[12] They are then driven into the eccrine sweat gland under hydrostatic pressure, which explains the correlation between cytokine concentration in sweat and plasma.[62,63] Sweat can be a suitable alternative for sampling IL-10 and small molecules that are challenging to isolate in serum or plasma due to the presence of large proteins.[64] Moreover, it offers potential for assessing the inflammatory state of older adults with chronic illnesses due to differential cytokine levels among age groups.

Besides continuous monitoring of biomarkers, it is equally important to assess the drug administration in real time during ambulatory care. Therapeutic drug monitoring (TDM) in plasma is a clinical practice to ensure the constant and optimal concentration of drugs in the blood to avoid any adverse effects of overdosing.[65] A few drugs have been reported to be found in sweat and the exact partitioning mechanism remains unclear.[66] For instance, the concentration of vancomycin, a highly monitored drug in a clinical setting, in sweat was around 0.2–2.5% that of blood.[67] Levodopa (L-dopa) which is mainly used to treat Parkinson's disorder, can lead to cognitive and motor dysfunctions if dosed inaccurately.[68] L-Dopa is excreted through sweat at a detectable micromolar range on standard dosage. Sweat L-dopa profile has been reported to correlate well with plasma concentration with a short time delay of around 10 min, indicating the feasibility of utilizing sweat for non-invasive continuous L-dopa monitoring.[69]

Sweat induction and sampling. The quantification of biomarkers in sweat primarily depends on the sweat generation mechanism and the sampling platform. Broadly, sweating can be categorized into active and passive. In active sweating, sweat is induced by a physical, thermal, or chemical external stimuli. Sweat generation *via* exercising has been a prevalent approach for performing on-body biomarker measurements, but intra- or inter-subject variability in body composition, exercise forms, and intensities can cause fluctuations in sweat rate.[70–72] Most importantly, this method is not ideal for the elderly or patients with existing medical conditions. Similarly, thermal induction is unsuitable as prolonged exposure to heat can be detrimental to the skin. Amongst the active sweating techniques, iontophoresis (IP) as depicted in Fig. 3A has garnered significant attention as it induces sweating when the body is at rest. IP is an FDA-approved method wherein a small current (0.2–0.5 mA cm^{-2}) is used to deliver cholinergic agents such as pilocarpine.[73–75] During a sedentary state, the sweat volume generated is around 0.1 nL min^{-1} per gland or less; thus the ability to achieve repeated and continuous sampling at reduced sample volume for a standard dose of pilocarpine is essential.[29] However, cholinergic agents, such as acetylcholine (ACh) or pilocarpine, have a short-term effect and are susceptible to acetylcholinesterase (AChE) hydrolysis; thus higher dosages of these stimulants need to be continuously supplied *via* IP for long-term sampling.[76] Simmers *et al.* reported prolonged and localized stimulation resulting in sweating for more than 24 hours using low dosages of carbachol, which is insensitive to AChE and has high muscarinic and nicotinic activity that is useful for wearable sensing.[77] Although IP provides a better alternative for sampling sweat than other active techniques, issues related to electrode stability, skin damage, and overdosing during extended stimulation need to be resolved for ambulatory monitoring.

Unlike active sweating, passive sweating simply involves the use of natural perspiration for sampling without the use of cumbersome and unsafe stimuli.[30] Fingertips are a painless and convenient route for sampling due to the abundance of sweat glands in the region that leads to a high natural perspiration rate.[78] Sweat sampling at the fingertip is mainly carried out using biocompatible, soft, and hydrophilic absorbent materials such as paper, sponge, textiles, or hydrogels. Hydrogels offer less resistance to sweat secretion and facilitate easy transport to the skin surface, preventing the local accumulation of sweat that builds the pressure barrier.[23,79] Rapid sweat glucose measurement within 60 seconds was successfully achieved

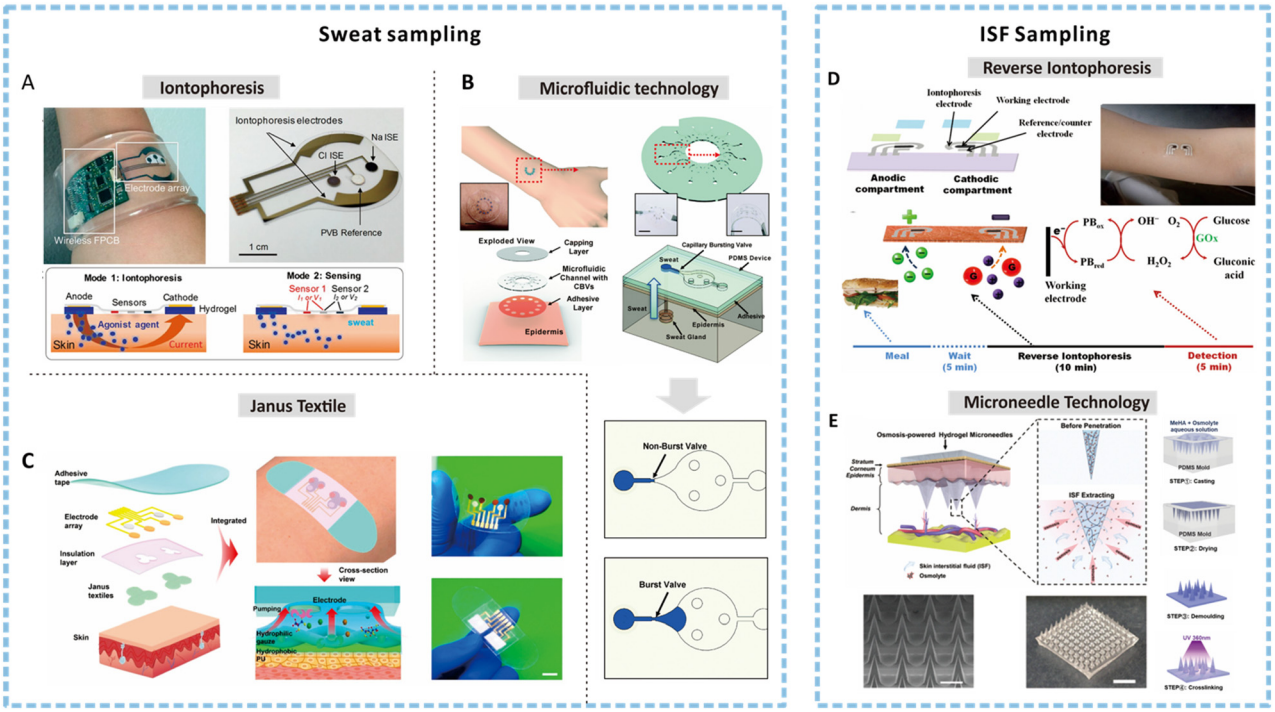

Fig. 3 Methods for sweat and ISF sampling. (A) An image of an integrated wearable platform for autonomous sweat extraction consisting of iontophoresis (mode 1) and sensing electrodes (mode 2). Reprinted with permission from Emaminejad *et al.*[75] Copyright© 2017 PNAS. (B) A soft and wearable microfluidic system for sweat sampling consisting of a capillary burst valve to control the flow of sweat in the channel. Reprinted with permission from Choi *et al.*[98] Copyright© 2017 The Royal Society of Chemistry. (C) Illustration depicting the exploded view of an integrated smart band with Janus textile to achieve self-pumping of sweat due to the wettability gradient. Reprinted with permission from He *et al.*[107] Copyright © 2020 American Chemical Society. (D) Schematic showing a reverse iontophoresis system integrated epidermal tattoo-based glucose sensing platform and the suggested time frame and processing for achieving glucose detection. Reprinted with permission from Bandodkar *et al.*[123] Copyright© 2014 American Chemical Society. (E) Schematic showing the osmosis-powered hydrogel microneedle (MN) array for ISF extraction and the corresponding fabrication process to develop a MN patch. Reprinted with permission from Zheng *et al.*[124] Copyright© 2020 WILEY-VCH Verlag GmbH & Co. KGaA, Weinheim.

by a touch-based sensor using porous polyvinyl alcohol (PVA) hydrogel for sweat sampling.[80] The porous hydrogel not only shortened the sampling time but also reduced the lag time. Several touch-based platforms have been developed over the years for the detection of various biomarkers and drugs.[81–83] Such sampling systems have certain drawbacks, such as contamination of a new sample with previously collected sweat and difficulty to quantify the sweat volume or rate. Besides, hydrogels are sensitive to environmental factors which can disrupt the network and affect the sweat transport.[30]

Sweat-based sensors can be suitable for ambulatory monitoring if they can achieve reliable and continuous biomarker measurements. However, on-skin sensors are prone to errors due to sweat evaporation, contamination, and dilution.[28,30] Microfluidic technology is one of the most efficient ways to sample natural sweat continuously that can be easily integrated with the sensing and other electronic components to develop a user-friendly interface.[84,85] Numerous soft microfluidic platforms based on PDMS have been introduced recently for this purpose.[86,87] These systems drive the flow of sweat by capillary forces, osmosis, or evaporation pumps to deliver the sweat to the detection chamber without external devices.[79] Microfluidic sampling devices based on capillary forces are the simplest. A microfluidic patch was introduced with a spiral microchannel based on PDMS that could hold a sample volume of 14 μL and last for 50 min for an average secretion rate of 10 nL min^{-1} per gland.[88] Although this device can continuously replenish the sweat, there is no regulation on the flow direction or the flow volume, which can lead to biofouling. The addition of capillary burst valves (CBVs), as shown in Fig. 3B, can passively control the flow direction of sweat by designing valves with a specific geometry to vary bursting pressures. In a multiple-valve design, the fluid will proceed through the valve with the lowest bursting pressure first and sequentially to other micro-reservoirs.[97,98] Moreover, hydrophilic treatment of the hydrophobic PDMS channels by plasma or UV or hydrophilic PVA coating can further assist in controlling the fluid flow. Such integrated microfluidic systems can allow sequential sampling and detect multiple biomarkers with minimal mixing.[99,100] However, sampling by capillary forces is lengthy in passive sweating scenarios, thus requiring the use of active sweating techniques such as exercising or heat application which are undesirable for ambulatory care.

Hydrogels can be used at the inlet of the microfluidic channel to create an osmotic pump to drive the sweat into the channels.[101] Additionally, it has been shown that the introduction of evaporation micropump-driven flow *via* micropores at the outlet can facilitate sweat flow rate of 0.24 μL min^{-1} without saturating the inlet or creating pressure imbalances.[102] Importantly, the flow rate can be controlled by tailoring the pore size, shape, and density. Current studies have only demonstrated the sampling efficiency of this concept and a separate peripheral workstation was used for detection.[103] To extend this concept for ambulatory monitoring, efficient integration of sensing, wireless, and powering components with this microfluidic technology is key. Moreover, a combination of capillary flow and evaporation micropump for sampling has the potential to achieve continuous and long-term sweat sampling passively.

Evidently, epidermal microfluidic technologies can address some of the major concerns associated with sweat sampling; however, they rely on complicated design structures and sophisticated fabrication equipment to control the flow of sweat.[104,105] Janus super-wettable materials have emerged as promising candidates to achieve on-demand fluidic manipulations. The wettability gradient arising as a result of the superhydrophobic and superhydrophilic side of a binary Janus membrane can lead to unidirectional transport of the sweat.[106] He *et al.* designed a flexible textile with Janus wettability by electrospinning hydrophobic polyurethane nanofibers on a superhydrophilic microfiber gauze, as shown in Fig. 3C.[107] The sweat droplets permeate the hydrophobic fiber and spread on the hydrophilic side that is integrated with electrochemical sensors for analyte measurements. Such a configuration significantly eliminates sweat retention and maintains a comfortable microenvironment for the users. The self-pumping capabilities of the Janus membrane have also been reported to enable real-time detection of ultralow volume of sweat around 0.15 μL.[108] Such systems hold great potential for multiplexed sensing of biomarkers in an ambulatory setting due to their low droplet usage, good microdroplet anchoring and sampling enrichment capabilities.

Challenges in sweat-enabled ambulatory monitoring. Although sweat has significant potential for non-invasive healthcare monitoring, several limitations still pose a challenge to its smooth translation to ambulatory care. One of the major challenges is the inherent >1000-fold dilution of most analytes in sweat compared to plasma.[12] A lack of understanding of the partitioning mechanisms for most of the biomarkers of interest in sweat makes it difficult to draw accurate interpretations and correlations with clinical significance. Passive sweat analysis in a sedentary state is more apt for ambulatory monitoring but the sweat secretion rate is in the sub-nanoliter range.[36] Moreover, sweat generation can be either increased or suppressed at rest in the case of patients with pre-existing conditions. Additionally, a standard approach to estimate and compensate for the effect of sweat rate fluctuation for various analytes has not been established yet. Intra- and inter-subject variability can also impact the sweat generation rate which can further complicate the correlations between sweat and blood.[17,23] Therefore, exploring a biofluid such as interstitial fluid (ISF) that eliminates most, if not all, of the concerns detailed above can be beneficial for the accurate prediction of health conditions and monitoring.

Interstitial fluid (ISF)

ISF is the most prevalent and accessible subcutaneous body fluid, constituting roughly 75% of the extracellular fluid in the human body. Almost 70% of ISF by volume is primarily present in the lowermost layer of the skin called the dermis. An interface exists between the dermis and the systemic blood circulation that drives the fluid flow *via* capillaries into the interstitial space.[31] ISF originates from the blood surrounding the tissues and the cells while delivering nutrients and signaling molecules. The exchange of biomarkers or analytes between the blood and ISF essentially takes place due to the existence of hydrostatic and osmotic pressure at the dermis–blood interface. Hence, the composition of ISF is very similar to that of blood and reflective of localized physiological information.[10,109] Understanding the role of capillary structure in the partitioning of analytes in ISF from blood is vital to gaining insight into relative concentrations of biomarkers of interest.

Partitioning of relevant biomarkers in ISF. The partitioning mechanism in ISF is dictated by the non-fenestrated nature of the continuous capillaries surrounding the dermis. The barrier function of these capillaries is regulated by tight junctions including cadherin junctions between the endothelial cells that allow the selective passage of analytes. The fundamental basis of the partitioning of biomarkers from blood to both sweat and ISF has many similarities. For instance, the dominating pathways involved in the transportation of analytes from blood to ISF occur in paracellular and transcellular mode.[32] Moreover, the size, charge, and properties of the biomarkers are key factors that determine their abundance in ISF relative to blood. However, a third partitioning pathway in the case of ISF involving vesicular transport of analytes through the cells has also been observed.[12] Molecular size influences the presence of biomarkers in interstitial fluid (ISF) due to cadherin junctions. Small hydrophilic analytes (>100 Da) partition into ISF *via* the paracellular route, while small hydrophobic analytes use the transcellular route.[32,110] Analytes smaller than 3 kDa diffuse easily through cadherin junctions, regardless of charge, mainly *via* paracellular diffusion. Tight junctions partially hinder analytes ranging from 3 to 70 kDa, allowing for both paracellular and transcellular partitioning. However, analytes larger than 70 kDa transfer *via* transcellular diffusion since they cannot pass through tight junctions. Charge and hydrophobicity also influence the blood-to-ISF partitioning. Proteins or drugs with neutral and

positively charged analytes can diffusive relatively free as compared to negatively charged ones (3–70 kDa), which are filtered by the negatively charged glycocalyx on the luminal surface of endothelial cells. Also, the dilution of larger analytes is much less compared to sweat due to the high surface-to-volume ratio and high density of the capillaries along with the force induced by blood.[111]

The concentration of electrolytes in ISF is equivalent to that of blood as the diffusion *via* the paracellular pathway is quite fast.[112] A wearable all-solid-state patch has been utilized for potentiometric detection of physiologically relevant levels of K^+ in ISF.[113] Glucose concentration in dermal ISF has been reported to be almost identical to plasma glucose under a steady state.[114,115] Glucose is a small hydrophilic molecule with a molecular size of 180 Da and thus partitions into ISF from plasma paracellularly with a short time delay (5–10 min).[32,116] Moreover, the rate of change of glucose concentration and the delay can also be affected by various physiological factors such as blood flow, tissue perfusion, and ISF permeability. Beyond physiological delay, the flux-limiting membrane of the CGM sensors further adds to the lag time, leading to sensor-specific delays.[117–119] Therefore, the scientific community has made efforts in recent years to address the lag time to achieve more precise and accurate glucose monitoring (further discussed in Section 3).

As mentioned before, measuring HB levels in diabetic patients can prove beneficial for diabetes management. It has been hypothesized that the plasma-to-ISF ratio for HB is close to 1 due to the similar molecular weight of ketone bodies and glucose.[120,121] Despite the limited data regarding the ISF levels, the concentration of ketone bodies has been reported to be around 2–3 mM during prolonged fasting. The rapid paracellular diffusion of the HB through the capillary interfaces can lead to good turnover in dermal ISF that is comparable to plasma. Urea is also a small analyte (60 Da) that is water soluble and highly diffusible.[122] Interstitial urea has also been reported to correlate well with the plasma urea in CKD patients. Interestingly, interstitial urea sampled from both the abdomen and the forearm displayed similar concentrations, implying that in equilibrium ISF behaves as a single compartment.[125] Creatinine is another small (116 Da) and neutral uremic toxin that is a key indicator of CKD progression. Epidermal interstitial-to-plasma ratio for creatinine was very close to unity in both healthy and non-hemodialysis CKD patients. UA (168 Da), which is negatively charged, was also reported to near-equivalent concentration in ISF and plasma. A probable reason is that its distribution is impacted by the Gibbs–Donnan equilibrium, *i.e.*, since plasma is more negatively charged, these molecules will be repelled towards the ISF. Additionally, the interstitial concentrations of urea, creatinine, and UA were higher in CKD patients relative to healthy individuals, suggesting that the measurement of uremic toxins in ISF can be carried out successfully in CKD patients.[126]

Signaling proteins such as cytokines (6–70 kDa) and cystatin C (13 kDa) are high molecular weight biomarkers.[127,128] The ISF/plasma ratio for these analytes has been reported to have an inverse logarithmic relationship with the weight due to the filtering by the tight junctions during paracellular diffusion.[12] It was found that the ISF/serum ratio for IL-1β was greater than 1, implying that IL-1β is primarily produced in ISF. In contrast, higher concentrations of TNF-α were reported in systemic circulation than in ISF. However, IL-6 has been observed to show a variable pattern in concentration in ISF *vs.* plasma over time.[129,130] Cystatin C, a positively charged smaller protein, has been found in significantly higher levels in ISF than in blood, suggesting that it is isolated within the interstitium. Further studies related to its abundant concentration in ISF and its relevance in early detection of kidney diseases are neccesary.[126]

ISF as a dermal fluid has gained considerable attention for therapeutic drug monitoring mainly due to two reasons: firstly, composition similarity between ISF and blood, and secondly, low protein content of ISF which suggests that drugs are likely present in their free or unbound form.[131] Kiang *et al.* conducted a pharmacokinetic study on the antibiotic profile in ISF for healthy and diseased individuals.[132] Penicillin showed lower concentrations in ISF compared to blood, while vancomycin exhibited a linear relationship between ISF and blood concentrations with a 30 minute lag time for steady-state distribution.[133] Monitoring L-dopa concentration in ISF has been explored, although blood-to-ISF correlation remains unclear. However, due to the molecular size and polarity, it has been hypothesized that L-dopa levels in ISF are similar to that of blood.[95] Recently, a highly sensitive interface monitored L-dopa down to 100 μM, demonstrating the feasibility of ISF for continuous monitoring of this drug.[134]

Sampling of ISF. ISF offers a substantial advantage over sweat because of little dilution of relevant analytes and close correlation to blood. It is minimally invasive and does not contain interfering biomolecules such as blood cells or induce blood clotting. However, ISF sampling is challenging mainly due to the low fluid volume, limited replenishment rate, and analyte filtration.[32] A biopsy involves the sampling of tissue to extract ISF in an off-body setting but it is invasive and prone to contamination.[135] The earliest implemented procedure method to extract ISF involved a nylon wick that is removed for post-analysis once it is saturated with ISF.[136] It is invasive, slow, can extract very low ISF volumes, and suffers from dilution. Alternatively, applying suction to the skin can extract fluid faster but the suction blister technique is inconsistent for continuous monitoring due to differences in large analyte composition compared to serum, making it unsuitable for certain biomarkers like cytokines or cystatin C. Microdialysis implants a semi-permeable membrane tubing in the dermis to extract ISF, allowing biomarker diffusion into a fluid inside the tube. However, it is unsuitable for ambulatory care as the biomarker composition in sampled ISF is often 5–10 times less than the physiological one.[10,32] Extraction of ISF using implantable subcutaneous sensors is

widely adopted in CGM systems, but they can be invasive and cause pain, infection, and scarring.[137] The above-mentioned techniques require long sampling times, expert training, healing time for injuries, and local anesthesia. Therefore, less invasive alternatives based on reverse iontophoresis (RI) and microneedle (MN) array (Fig. 3D and E) for ISF extraction are beneficial for continuous biomarker monitoring in ambulatory care.[50,123,124] RI applies low electrical current to facilitate ion flow across the skin without puncturing or damaging it. When the electric field is applied, the charged ions and some neutral analytes move to the cathode due to the negative charge of the skin. RI causes the electroosmotic flow of ISF through the flow of ions and the formation of ionic current due to sodium ions leading to its extraction. However, this technique is limited to small cationic species. The effectiveness of RI depends on factors like current amplitude, time, pH, skin temperature, and skin permeability. Since the flow occurs through the paracellular route, the sampled ISF differs from physiological ISF due to the filtering effect of tight junctions, similar to sweat, resulting in dilution.[32,138] Therefore, it is necessary to understand its correlation to the true ISF and blood content. Moreover, prolonged extraction of ISF using RI has been linked to skin irritation making it inept at the current stage for ambulatory monitoring. MN array is an emerging technology to extract ISF in a minimally invasive manner with immense potential for continuous monitoring. Unlike invasive injections or needles for blood sampling, MN array offers a painless, convenient method that enhances patient compliance.[34] MN arrays are made of micron-size needle-like projections that can easily interface with skin to facilitate the transport of the fluid. Any indentations created after the application of the MN array are readily healed. MN arrays can be solid, hollow, porous, dissolving, and hydrogel-based. Some of the literature provides a very detailed account of these technologies[10,139] Solid and dissolving MN are mainly for single-time use as they require additional accessories for the collection and analysis of ISF.[140] Porous, hollow, and hydrogel-based integrated MN arrays have been exploited relatively more for continuous biomarker detection with simultaneous extraction and detection.[141–143] A hollow MN array integrated with an enzymatic detection platform is beneficial as the imbalance created due to analyte consumption leads to continuous diffusion of ISF.[144] Moreover, MN arrays facilitate the direct quantification of biomarkers.[10,31] From an ambulatory care point of view, soft, compliant, and highly biocompatible hydrogel-based MN interfaces are relatively more suitable. However, this early-stage approach is limited to the extraction of specific biomarkers due to the charge and mesh size of the hydrogel network, and the sub-microliter volumes extracted are insufficient for diagnostics.[145] Overall, MN-based ISF sampling and analysis show promise for rapid and less invasive localized screening of chronic diseases and drug monitoring, but further research on stability, reproducibility, and large-scale production is needed for clinical adoption.

Challenges in ISF-enabled ambulatory monitoring. ISF is a promising biofluid for minimally invasive, rapid, continuous, and accurate monitoring of biomarkers in an ambulatory setting. Extraction of true dermal ISF is a major challenge as the high resistivity of the dermis restricts the flow of the fluid to achieve an optimal sampling volume and sampling rate. Another issue is that ISF sampling can disrupt the epidermis, thereby inducing an immune response and disturbing the concentration of analytes in the ISF and its correlation with the blood.[32] Large molecules such as proteins, cytokines, and several drugs of interest are present in much lower concentrations than in blood, hence detection of these biomarkers remains an obstacle.[31]

3. Sweat- and ISF-based biosensors for ambulatory care

3.1 Chronic disease monitoring

Diabetes. Diabetes is a prevalent chronic metabolic disorder that affects millions of individuals, leading to potential cardiovascular or chronic kidney disease due to inadequate regulation of blood glucose levels.[137,146] Prediabetes, with high but below-diabetic blood sugar levels, often goes undiagnosed and untreated for years.[150,151] The screening procedures require frequent visits to hospitals or the use of costly and invasive finger-pricking glucometers several times a day which is cumbersome and prone to infection.[152,153] Continuous and minimally invasive glucose monitoring systems can enable early detection and real-time feedback for glycemic control, but existing non-invasive technologies based on optical, acoustical, electric, and microwave techniques lack sensitivity and selectivity and are susceptible to physiological or environmental variations.[154] Wearable platforms using dermal fluids are promising alternatives for less invasive and more accurate glucose monitoring.

The feasibility of using sweat glucose for diagnosing prediabetes or diabetes remains controversial due to inconsistent correlations with blood glucose.[52,155] Understanding glucose partitioning, lag times, sweat rate effects, composition, and variations is crucial to establish universal screening thresholds.[17] Also, sweat sampling, contamination, sweat gland activation, pH deviations, and skin temperature need to be considered. Besides, the low concentration of glucose in sweat compared to blood with a dilution factor of 100-fold demands a highly sensitive detection platform.[28,156] Therefore, further research in materials, sweat sampling, and sensitive sensing mechanisms is crucial to overcome these challenges. To date, wearable sweat glucose monitoring sensors based on colorimetric and electrochemical methods have been developed.[156–159] Colorimetric sensing is a practical and affordable method for sweat analysis, suitable for self-monitoring.[160,161] Although colorimetric sensors overall suffer from low limit of detection (LOD), a filter paper-based wearable glucose sensor with a LOD of 0.01 mM useful for hypoglycemia was reported.[162]

However, such methods are often prone to uneven coloring and require frequent replacements. A recent microfluidic platform offers multimodal functionality and lighting-independent colorimetric sensing of glucose, lactate, chloride, pH, and sweat temperature.[160] Field study during exercise demonstrated its capability of ambulatory care for identifying prediabetic conditions wherein sweat glucose level changed with diet and exercise.

Electrochemical sensors are widely adapted and feasible for real-time, accurate, and long-term diabetes management.[163–166] Skin-integrated electrochemical sensors can facilitate real-time sweat glucose analysis, but the use of batteries, electronics for wireless transmission, and external displays impact the form factor and cost. Zhao *et al.* developed an integrated, self-powered smartwatch powered by amorphous silicon (a-Si) photovoltaic cells and a rechargeable zinc–manganese oxide ($Zn–MnO_2$) battery (Fig. 4A).[147] The enzymatic electrochemical sweat glucose sensor displayed appreciable sensitivity and provided real-time alerts corresponding to low (15–30 μM), medium (50–100 μM), and high (150 μM) levels. This real-time feedback is valuable for managing the health of hypoglycemic, prediabetic, and diabetic people. Enzymatic electrochemical glucose sensors primarily use glucose oxidase (GOx) which is prone to instability due to pH and temperature changes in sweat that can impact catalytic activity.[167] Hence, sweat glucose, pH, temperature, and humidity measurements can be integrated into the glucose sensor for real time correction. Correspondingly, significant efforts are being directed towards the non-enzymatic approach for glucose sensing in sweat.[168,169] These sensors are mostly based on transition metals or metal oxide and operated under alkaline conditions (pH >11), but sweat has a neutral pH which can hamper the operation stability and accuracy of these. Therefore studies have been carried out to enable non-enzymatic glucose monitoring in this pH range.[170–172]

The ISF glucose concentration is highly correlated with blood glucose both during steady state and glycemic conditions, making it a reliable alternative for sensitive and accurate data acquisition.[173–175] However, the time delay between changes in ISF and blood glucose, influenced by physiological conditions, remains a significant challenge.[117] Currently, implantable CGM systems based on ISF are the only clinically implemented devices with a huge market

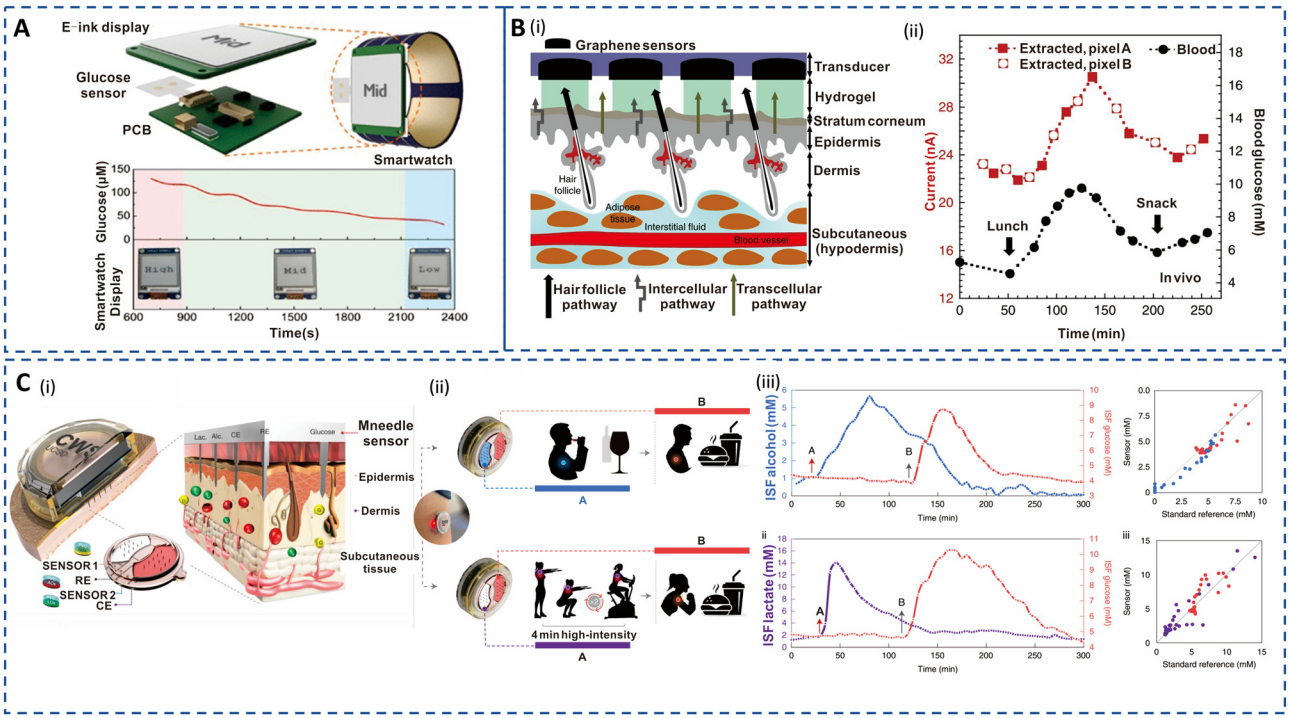

Fig. 4 Sweat- and ISF-enabled detection platforms for diabetes management. (A) Illustration of self-powered smart integrated sweat glucose sensors with electronic ink (E-ink) display for real-time monitoring (top). Reprinted with permission from Zhao *et al.*[147] Copyright© 2019 American Chemical Society. (B) (i) Pixel array and preferential glucose routes along the hair follicles. (ii) *In vivo* continuous glucose monitoring profiles performed for 6 h during lunch and snack consumption. Red curve depicts ISF glucose extracted from two pixels (A and B) in tandem. Black curve depicts blood glucose measurement using a commercial glucose meter. Reprinted with permission from Lipani *et al.*[148] Copyright© 2018 Springer Nature. (C) (i) Cross section of the ISF-enabled wearable device with microneedles piercing the skin and the schematics of the microelectrodes' configuration for multiple analyte detection. (ii) Performance study of the sensor during wine consumption event followed by a meal consumption (top) and a high-intensity workout followed by full meal consumption (bottom) for alcohol–glucose and lactate–glucose sensing, respectively. (iii) Plot of ISF alcohol and glucose measurements (top left) and the corresponding standard breath analyser and blood glucose measurement (top right). Plot of ISF lactate and glucose measurements (bottom left) and the corresponding standard blood lactate and blood glucose measurement (bottom right). Reprinted with permission from Tehrani *et al.*[149] Copyright© 2022 Springer Nature.

acceptance. Continuous monitoring sensors such as Dexcom G6 (Dexcom, San Diego, USA) and Freestyle Libre 2 (Abbott, Chicago, USA) are the dominant players among commercialized subcutaneous CGM devices.[176,177] However, less invasive monitoring alternatives based on RI and MN array for ISF extraction are desired for glucose monitoring in ambulatory care.

Glucowatch G2 Biographer, the first commercial device based on RI for monitoring glucose for up to 12 h based on ISF, received US-FDA approval in 2001. However, it was discontinued as time delay, prolonged warm-up period, and frequent blood sampling for calibration led to skin irritation and blisters.[178,179] Another limitation of RI is the dilution of the extracted glucose due to large skin area extraction, requiring the use of finger prick sampling for calibration.

Hence, recent efforts have focused on improving the user experience.[180] A transdermal patch with a path-selective pixel array of Pt-decorated graphene electrodes was introduced to address the dilution issue (Fig. 4B(i)). The patch utilized the hair follicles' preferential pathway for electroosmotic flow, which resulted in a glucose flux of 3.5 nmol mA^{-1} h^{-1} at ISF concentration of 10 mM. As observed in Fig. 4B(ii), the RI-extracted ISF closely followed the blood glucose profile with 15 min lag time in *in vivo* testing. This method enabled calibration-free measurement across the hypo- to hyperglycemic range, offering a non-invasive approach for diabetes management. RI efficiency is also susceptible to skin resistance changes occurring during perspiration; thus, critical and selective evaluation of glucose in ISF is key for accurate glycemic control. Large-scale clinical trials and testing are needed for potential commercialization and wider adoption of this technology.[148]

Clinical studies have reported that glucose detection using MN arrays is associated with a low pain score and has been verified for patient acceptability and clinical efficacy.[181] Tehrani *et al.* introduced an integrated wireless solution for continuous and simultaneous measurement of multiple analytes based on poly(methyl methacrylate) MN microelectrodes (Fig. 4C(i)).[149] The sensor successfully captured multiple lag-free biomarker profiles during wine and food consumption and workout (Fig. 4C(ii)). Importantly, the data were well correlated with standard measurements as shown in Fig. 4C(iii). This technology underscores the accuracy of MN for ISF-based glucose detection and overcomes the practical limitations associated with current CGMs. Soft, compliant, and biocompatible hydrogel-based MN interfaces are desirable features for ambulatory diabetes management. Wang *et al.* developed a highly sensitive and responsive smart glucose-responsive hydrogel.[182] The blood glucose levels in diabetic mice showed a strong correlation with quantitative readouts corresponding to the glucose concentrations detected by the glucose-responsive MN array. Although this approach achieved rapid and minimally invasive measurements, the characterization results were recorded using a CCD camera which is not practical for wearable formats. Thus, hydrogel-based MN detection platforms with intuitive visible read-out and controlled insulin delivery are promising for diabetes theranostics, with the possibility to apply these sensors for prediabetic and type 1 and 2 diabetic patients.

Diabetic ketoacidosis (DKA) is a severe diabetic complication arising from insufficient insulin levels in the body, thereby resulting in an excess of ketone bodies.[183,184] The continuous monitoring of ketone bodies has not been addressed despite significant advancements in new-generation CGM devices capable of sensing glucose directly in the ISF. Teymourian *et al.* demonstrated the capability of a hollow MN array for real-time electrochemical monitoring of HB levels in ISF for the first time in 2020.[121] This method relied on a β-hydroxybutyrate dehydrogenase (HBD) enzymatic reaction for sensitive and selective HB detection, exhibiting a LOD of 50 μM, prolonged operation stability, and antifouling characteristics in artificial ISF. The same group recently developed a non-invasive and rapid touch-based dual biosensor to track dynamic rest sweat HB and glucose on the fingertip using a single-strip substrate.[54] This biosensor demonstrated a personalized HB dose–response relationship and a correlation between sweat and capillary blood HB levels in healthy human subjects after taking commercial ketone supplements. The development of dermal fluid-based biosensors capable of simultaneous and long-term glucose and ketone measurement is an area of active interest aimed toward enhanced diabetes management.

Chronic kidney disease. Chronic kidney disease (CKD) is a condition that leads to gradual loss of kidney function, affecting 10% of adults worldwide, especially the elderly. CKD is often asymptomatic initially, and the slow progression of kidney failure takes months to decades.[187,188] CKD is typically assessed by monitoring changes in metabolites (urea and creatinine) and electrolytes (K^+) that reflect renal function.[90] Glomerular filtration rate (GFR) calculated from creatinine concentration indicates the severity of kidney disease, while blood urea nitrogen provides information about renal tubular function. Decreased kidney function leads to elevated levels of these biomarkers in the blood.[189–191] In young adult men and women, the typical value of GFR is around 125 mL min^{-1}/1.73 m^2, whereas values less than 15 mL min^{-1}/1.73 m^2 signify kidney failure. However, GFR-based diagnostics can only be used for stage 3–4 CKD patients, and failure to slow down the progression can lead to death.[192] The current standard for kidney disease screening involves costly laboratory tests on blood and urine samples, requiring trained professionals and specialized facilities. Serum creatinine monitoring is a gold standard in CKD management but requires frequent cumbersome sample collection, and it is prone to pH and temperature changes and contamination due to interfering biomolecules.[49,55,90] Therefore, ambulatory monitoring of CKD biomarkers in accessible dermal fluids such as sweat and ISF can overcome the limitations of serum-based sampling.

Sweat creatinine and urea levels are higher in CKD patients than in healthy controls.[56,58] Thus, detection of

these biomarkers in sweat *via* colorimetric or electrochemical approaches is currently being studied extensively.[193,194] Additionally, sweat pH is crucial for CKD as the dehydration status of an individual has been linked to metabolic alkalosis. Zhang *et al.* developed an epidermal integrated microfluidic device to simultaneously measure creatinine, urea, and pH relying on enzymatic detection and colorimetric readout, for kidney disease screening and monitoring as shown in Fig. 5A(i and ii).[60] The concentrations of the biomarkers correlated well with standard lab-based tests as depicted in Fig. 5A(iii). Moreover, it allowed for patient-friendly capture of sweat without physical exertion or pharmacological stimulation. The development of multicomponent integrated sensors to monitor physical, biological, and chemical signals for carefree living of patients is an emerging area for research.[195] Despite the development of advanced wireless systems, the requirement of large power supplies and maintenance costs hamper their applicability. Zhao *et al.* introduced a self-powered wearable sensor to successfully monitor glucose, creatinine, and lactic acid in sweat while capturing body motion using an enzymatically modified conductive and stretchable fiber-based triboelectric nanogenerator (F-TENG).[196] This F-TENG can perform real-time metabolic profiling in sweat by detecting glucose and creatinine with a sensitivity similar to that of commercial meters without relying on an external power source. However, the sensitivity for lactic acid was affected by interfering biomolecules in sweat. Nonetheless, this portable platform has significant potential applications in medical rehabilitation and early emergency intervention. It should be noted that enzymatic reactions used for sweat urea sensing may degrade over time, leading to reproducibility issues during long-term monitoring. Recently, an epidermal optofluidic sensor based on single-band Raman analysis

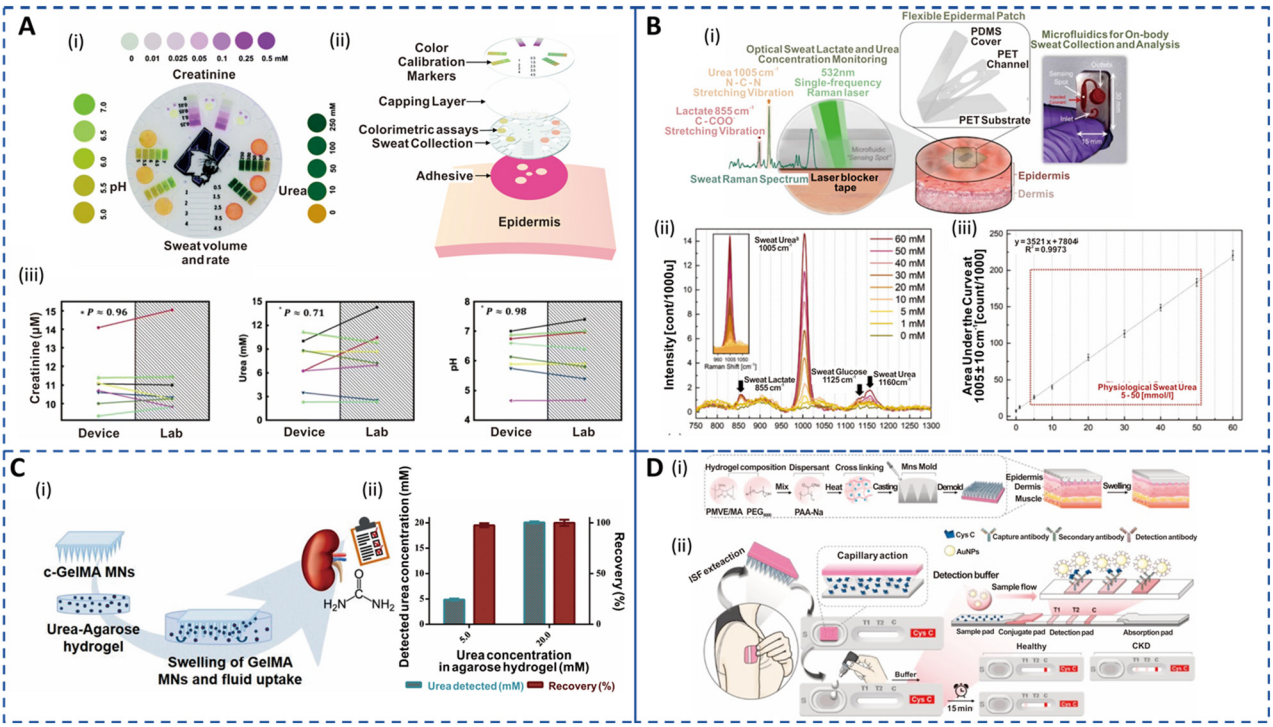

Fig. 5 Sweat- and ISF-enabled detection platforms for CKD management. (A) (i) Colorimetric detection platform depicting the spectrum of colors corresponding to the relevant pH range (left), creatinine (top) and urea (right) in sweat. (ii) Exploded image illustrating the various components of the epidermal sensor. (iii) Biomarker concentrations in sweat measured using an epidermal sensor against laboratory-based analysis (n = 8). Data points with the same color belong to the same test. Reprinted with permission from Zhang *et al.*[60] Copyright© 2019 Royal Society of Chemistry. (B) (i) Schematic of the optofluidic sensor for sweat urea and lactate monitoring. The illustration shows the exploded image of the epidermal patch (center). The zoomed-in illustration (left) shows the microfluidic sensor when the Raman laser is active and the corresponding spectral bands for sweat urea and lactate. A laser blocker tape is used to block the out-of-focus beams from directly entering the skin to avoid any hazardous effects. An image of the fabricated optofluidic chip for sweat analysis (right). (ii) Sweat Raman spectra for various urea concentrations depicting a sweat lactate Raman band at 855 cm^{-1}, urea at 1005 cm^{-1} and 1160 cm^{-1}, and glucose at 1125 cm^{-1}. The inset shows the area under the curve (AUC) of the characteristic sweat urea band. (iii) Physiological sweat urea calibration curve in the 5–50 mmol l^{-1} range with a limit of detection of 0.47. Reprinted with permission from Golparvar *et al.*[185] Copyright© 2023 Elsevier. (C) (i) Schematic demonstrating the *in vitro* swelling and ISF extraction of cross-linked gelatin methacryloyl (c-GelMA) MNs in an agarose model system for non-invasive urea monitoring. (ii) Plot depicting the correlation of the detected urea concentration and recovery efficiency of the c-GelMA system in spiked agarose models mimicking the normal and CKD states. Reprinted with permission from Fonseca *et al.*[186] Copyright© 2020 Wiley-VCH GmbH. (D) (i) Fabrication procedure of the epidermal hydrogel MN patch (HMNP). (ii) Schematic showing the proposed approach for blood-free detection of Cys C. The HMNP patch is placed on the skin for ISF extraction for 5 min and then placed on the lateral flow strip for antibody detection, delivering a visual readout for heathy and CKD patients in 15 min. Reprinted with permission from Chen *et al.*[94] Copyright© 2022 Elsevier.

(Fig. 5B(i)) was developed to quantify sweat lactate and urea in a large dynamic range (0 to 270 mmol l^{-1}).[185] The platform consisted of a flexible microfluidic device with low Raman activity placed on the skin. The proposed single-band Raman spectroscopy eliminated the inherent limitations of poor shelf life, low reproducibility, and complex fabrication procedures of surface Raman-based methods and facilitated label-free portable detection. Moreover, this approach is advantageous for the analysis of biomolecules in sweat as it has a simpler Raman spectrum compared to blood. Fig. 5B(ii and iii) show the Raman spectra for sweat with varying urea concentrations with area under the curve characteristic urea band displaying a linear correlation with the concentration change. The device offered selective urea and lactate measurements in human sweat (thermal and exercise inducement) without interference from analytes such as uric acid and creatinine. Most importantly, the platform achieved highly reproducible and stable biomarker detection in artificial sweat for 3 months, demonstrating its potential for multiplexed ambulatory monitoring.

Urea and creatinine levels in ISF are highly correlated to those in blood and serum.[126] Continuous monitoring of blood urea levels throughout is essential for understanding urea kinetics and evaluating the effectiveness of hemodialysis. Iontophoretically extracted urea can rapidly reflect changes in plasma urea following hemodialysis in CKD patient. This implies that non-invasive urea detection is useful not only for CKD diagnosis but also for assessing dialysis efficiency.[197] The potential of RI for ISF urea detection was explored using a screen-printed potentiometric sensor wherein urease was immobilized on a micro-structured polypyrene (PPy) matrix that displayed excellent linearity in the range of 10–5000 mM with stable performance for up to 40 days.[198] However, calibration was required, and a few subjects experienced tingling sensations and erythema. MN extraction results in ISF that is more indicative of true physiological ISF than RI. It has been demonstrated that gold microneedles (AuMNs) functionalized with a polymeric mediator and urease enzyme can be successfully utilized to determine urea in ISF.[199] Their performance was evaluated in artificial ISF and alginate epidermal/skin mimic spiked with urea, achieving detection in the range of 50–2500 mM with a sensitivity of 52 nA mM^{-1} and 31 nA mM^{-1}, respectively. However, this platform is limited by the low chronoamperometric response and a lack of *in vivo* measurements to validate the clinical efficacy of metal-based MNs for long-term monitoring. Fonseca *et al.* investigated the potential of swellable crosslinked gelatin methacryloyl (c-GelMA) hydrogel-based MNs towards PoC monitoring of kidney disorders as illustrated in Fig. 5C(i).[186] The fabricated biocompatible MNs exhibited good insertion ability to sample ISF for real-world applications and successfully quantified urea at normal (5 mM) and CKD state (20 mM) on a spiked agarose hydrogel model with excellent recovery efficiency as shown in Fig. 5C(ii). Although, the swellable characteristic is essential for ISF sampling the MNs reached 63% of volume capacity within 4 min, implying that this system is apt for short-term measurements. This technology has potential for clinically safe CKD biomarker monitoring due to its non-invasive character.

Cys C has been proposed as a promising biomarker for the early diagnosis of acute kidney injury and CKD as it is less affected by body composition or the age of the patients and has been reported to be more accurate than creatinine for eGFR estimation.[200–202] Most traditional methods for Cys C detection are immunoassays that utilize serum and are time-consuming and costly to perform. Chen *et al.* integrated a hydrogel MN patch(HMNP) with a lateral flow cassette ($LFC_{Cys\ C}$) for at-home rapid detection of Cys C in dermal ISF within 25 min (Fig. 5D(i and ii)).[94] A crosslinker (polyethylene glycol 8000: PEG_{8000}) and an absorbent material (sodium polyacrylate PAA-Na) were introduced in the poly(methyl vinyl ether-alt-maleic acid (PMVE/MA))-based hydrogel MNs to tailor the swelling characteristics for efficient extraction. The HMNP is first pressed on the skin for 5 min for ISF extraction and then attached to the $LFC_{Cys\ C}$ sample port for antibody-based detection in a blood-free PoC kit displaying a distinctive visual readout for healthy and CKD subjects as depicted in Fig. 5D(iii). In addition, the patch efficiently extracted biomolecules in the range of 0.5–67 kDa, which suggests its feasibility for extracting Cys C from ISF. This PoC platform could clearly distinguish between healthy and CKD rats. Such MN technologies support the feasibility of utilizing ISF for the detection of various CKD biomarkers. Furthermore, creatinine monitoring to date has been limited to body fluids such as urine and saliva;[49] thus, the development of biosensors for creatinine detection in ISF has a vast scope.

3.2 Chronic inflammation monitoring

Inflammatory diseases encompass a wide range of disorders caused by various factors including infections, immune system abnormalities, cell damage, neurological disorders, toxic compounds, *etc.* Inflammation is the body's response to injuries by inducing a complex cascade to initiate tissue healing by recruiting leukocytes, pro-inflammatory cytokines and chemical mediators, and acute-phase proteins. While acute inflammation is a normal process for healing, chronic inflammation can contribute to the development of various illnesses such as cardiovascular diseases, diabetes, CKD, cancer, rheumatoid arthritis, and neurodegenerative disorders.[203–206] The detection of inflammatory biomarkers is key for diagnosis, prognosis, and selection of appropriate therapy of chronic inflammatory disorders. Traditionally, enzyme-linked immunosorbent assay (ELISA) and polymerase chain reaction (PCR) are used to quantify these biomarkers.[207,208] Although sensitive and specific, these techniques are time-consuming and limited to clinical settings. Real-time detection of potential inflammatory biomarkers for timely prediction of chronic inflammation progression is a major challenge.

Cytokines are significant mediators responsible for the regulation of immunological and inflammatory responses. Quantifying cytokines is clinically significant for understanding immunological and inflammatory responses. Blood analysis of cytokines aids the diagnosis, but their short half-lives and degradation during sampling can lead to false negatives.[61] Furthermore, invasive measurements cannot continuously track inflammation flares in real time. Hence, non-invasive analysis of dermal fluids opens up new opportunities for chronic inflammation management. Recent studies have explored detecting cytokines in human sweat for various disorders. Upasham *et al.* developed a flexible wearable sweat sensor to study the relationship between endocrine and inflammation pathways on exposure to stress.[209] The platform, used to detect cortisol and TNF-α, incorporated a biocompatible hydrophilic nanoporous membrane to facilitate the detection of ultralow volume (3 μL) of passive sweat *via* rapid wicking action. The sensor successfully quantified TNF-α in sweat in a linear dynamic range of 1–1000 pg ml^{-1}, which is suitable for diagnostic purposes. A wearable and non-invasive platform termed SWEATSENSER was introduced for inflammatory bowel disease (IBD) management.[210] Real-time, multiplex, and continuous detection of biomarkers IL-β and C-reactive protein (CRP) in sweat was carried out to monitor inflammation flare-ups. The sensor exhibited high sensitivity in spiked sweat and showed a strong correlation with standard ELISA measurements. Moreover, the SWEATSENSER maintained stable on-body measurements for over 30 hours with minimal variation in IL-1 β levels amongst healthy subjects. This developed SWEATSENSER platform as depicted in Fig. 6A(i) was further employed to detect flu directly in passive sweat by real-time monitoring of various inflammatory cytokines (IL-6, IL-8, IL-10, and TNF-α).[62] As shown in Fig. 6A(ii), the platform could successfully capture the temporal dynamic changes in cytokine levels from early pathogen attack to the recovery phase during infection. In addition, the group recently demonstrated the viability of monitoring ultralow levels of sweat IFN-γ, an important inflammatory biomarker for cancer, to aid clinicians in disease management.[211] However, more comprehensive studies for inflammatory biomarkers on diseased cohorts based on integrated sampling and sensing systems and long-lasting sensors are needed.

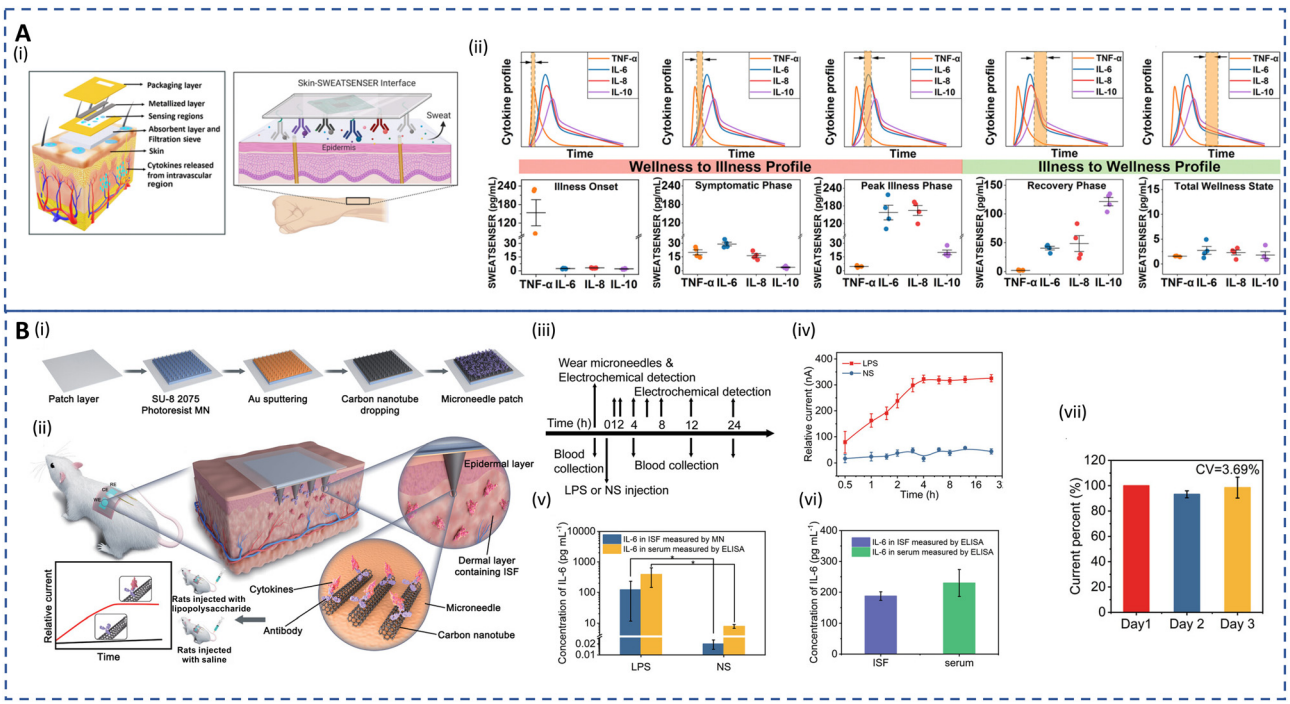

Fig. 6 Sweat- and ISF-enabled detection platforms for chronic inflammation monitoring. (A) (i) Schematic depicting the exploded image (left) of the skin–SWEATSENSER interface which is functionalized with specific antibodies (right) for cytokine detection. (ii) Plots showing the SWEATSENSER's capability to accurately monitor biomarker levels across different stages of infection. Temporal profiles of inflammatory biomarkers from wellness to recovery (top) and the corresponding whisker plots for the reported levels of biomarkers (bottom). The band marked with double arrows in the temporal profile plots represent the time snapshot of the cytokine profile during various stages. Reprinted with permission from Jagannath *et al.*[62] Copyright© 2021 Wiley-VCH GmbH. (B) (i) Illustration showing the fabrication of the wearable MN patch. (ii) Schematic showing the application of the MN patch on the skin and the corresponding detection mechanism for *in vivo* cytokine monitoring. (iii) Workflow demonstrating the lipopolysaccharide (LPS) or normal saline (NS) injection, blood collection, and MN detection for real-time *in vivo* cytokine monitoring for 24 h. (iv) Real-time measurement for 24 h on rats using the MN patch. (v) Comparative analysis for detection of IL-6 in rats of the MN patch and ELISA. For (iv) and (v), error bars indicate mean ± SEM, n = 5 per group. (vi) IL-6 detection in ISF *vs.* serum using ELISA after 4 h injection. (vii) Sensitivity of the MN patch on rats for 3 days where current percent = $current_{day\ n}/current_{day\ 1} \times 100\%$, n = 3, 4, and 5. For (vi) and (vii), error bars indicate mean ± SEM, n = 3. Reprinted with permission from Xu *et al.*[22] Copyright © 2023 Wiley-VCH GmbH.

In dermal ISF, concentrations of inflammatory biomarkers are often lower than in blood.[129] Additionally, the dense tissue environment impairs analyte–antibody binding kinetics, which impacts the sensing performance. Z. Wang *et al.* developed a biocompatible and pain-free microneedle patch for fast sampling and direct quantification of protein biomarkers in ISF.[130] An ultrabright fluorescent nanolabel termed plasmonic flour was used to enhance the sensitivity of the MN-based immunoassay, overcoming challenges of conventional ELISA in terms of sensitivity and multiplexity. The assay showed 160-fold higher sensitivity compared to standard ELISA when assessing mouse IL-6, and good qualitative correlation between levels in ISF and serum. A novel electrochemical approach combining molecularly imprinted polymers (MIPs) and MN arrays was utilized for PoC testing of IL-6.[212] This transdermal sensor detected IL-6 levels as low as 1 pg mL^{-1} in artificial ISF. In diseases such as COVID-19, cancer, and sepsis, a sudden dysregulation of inflammatory cytokines can lead to a life-threatening cytokine storm. Most recent investigations have used an *in vivo* capture and *in vitro* analysis two-step approach to find biomarkers in sweat and ISF, which are time-consuming and error prone. Therefore, J. Xu developed an integrated wearable MN patch for real-time monitoring of a cytokine storm *in vivo*.[22] Fig. 6B(i and ii) show the fabrication process of the MN patch and the cytokine detection strategy in rats. The MNs were functionalized with conductive carbon nanotubes (CNTs) to facilitate the capture of cytokines in ISF. Antigen–antibody-specific binding takes place in seconds, reaching a stable state in a few minutes. Thus, the patch can measure real-time changes in cytokine levels with a short lag. This wearable system displayed an LOD of 0.54 pg ml^{-1}. The workflow and the corresponding current response for real-time measurement of LPS and NS injection are depicted in Fig. 6B(iii and iv). The platform was able to achieve continuous monitoring for 24 h *in vivo* with a quick response corresponding to cytokine increase within several hours (1–4 h). In all groups of rats, MNs had shown excellent qualitative agreement with ELISA as seen in Fig. 6B(v). Additionally, 4 hours after LPS injection, the IL-6 levels in the collected ISF and blood both displayed similar results as determined by ELISA (Fig. 6B(iv)). Fig. 6B(vii) shows that the current signal stayed relatively stable for 3 days with a CV of 3.69% during *in vivo* analysis. Similar fully integrated systems utilizing ISF can help determine the immune status of patients and provide a rapid, accurate, and appropriate treatment in ambulatory settings.

3.3 Therapeutic drug monitoring (TDM)

A crucial aspect of ambulatory care is to minimize healthcare costs through preventive medicine and TDM in outpatient settings.[214] Desirable TDM involves closely monitoring drug levels in biofluids, like plasma, to personalize pharmacotherapy, minimize drug toxicity, and fine-tune dosage effectiveness.[131] TDM is particularly important for drugs with narrow therapeutic windows, where small dosage variations can have significant effects, such as in antibiotic administration.[215,216] Furthermore, the effectiveness and safety of a drug are also affected by wide interpatient variations in drug absorption and metabolism.[217] Currently, TDM relies on frequent blood tests and is limited mainly due to the cost and complexities associated with lab-based techniques. Besides, interactions of drugs with plasma proteins lead to inaccurate measurements. Urine is also used for drug analysis due to its non-invasive nature and quantifiable drug concentrations. However, the dependence of drug concentration on the urine volume and tampering with urine samples undermines the efficacy of the urine-based drug testing.[34,215,218] A facile platform for continuous TDM can eliminate several clinical setbacks of the current approaches.

Alternative matrices, such as sweat and ISF, that allow real-time and non-invasive ambulatory monitoring could considerably improve patient outcomes. Because these matrices reflect unbound concentrations in blood, no extra processes are required to identify clinically significant free drug levels. Sweat-based TDM is the earliest method that dates back to the 19th century and its feasibility has been well proven for drug pharmacokinetic studies.[132,219,220] However, drug concentrations are ultralow and challenging to detect. Recently, electrochemical sensors have witnessed significant growth in drug screening and serve as promising alternatives to chromatography and spectrometry in terms of sensitivity and selectivity.[221] Tai *et al.* developed an electrochemical wearable sweatband for non-invasive L-dopa detection for Parkinson's disease management (Fig. 7A(i–iv)).[68] The sensors, which incorporated gold dendritic nanostructures on the electrodes, displayed a LOD of 1 μM in sweat. Moreover, its long-term stability was enhanced using glutaraldehyde to immobilize the tyrosinase enzyme for L-dopa oxidation. The sweatband was employed to monitor the sweat profile of L-dopa during both iontophoresis and exercise-induced sweat after fava bean intake. In the case of iontophoresis, when the subject consumes only fava beans, the observed sweat levodopa level increases by 6.6 μM at 47 min and then subsequently declines as depicted in Fig. 7A(v). Fig. 7A(vi) shows that if the subject consumes a sandwich before fava bean intake, a slight delay of 13 min in the pharmacokinetic peak time is observed as expected. The exercise-induced sweat analysis followed the same trend for the pharmacokinetic profile as mentioned above during exercise-induced sweat. This showcases the potential benefits of the wearable sweatband in continuously monitoring the dynamic metabolic rate of L-dopa, highlighting its applicability for dosage optimization.

Nevertheless, continuously produced resting sweat is a more desired form of sweat for long-term monitoring compared to short-term chemically or exercise-induced sweat. In addition, the sedentary sweat secretion rates can be associated with various underlying health conditions. Nyein *et al.* designed a wearable patch for continuous analysis of

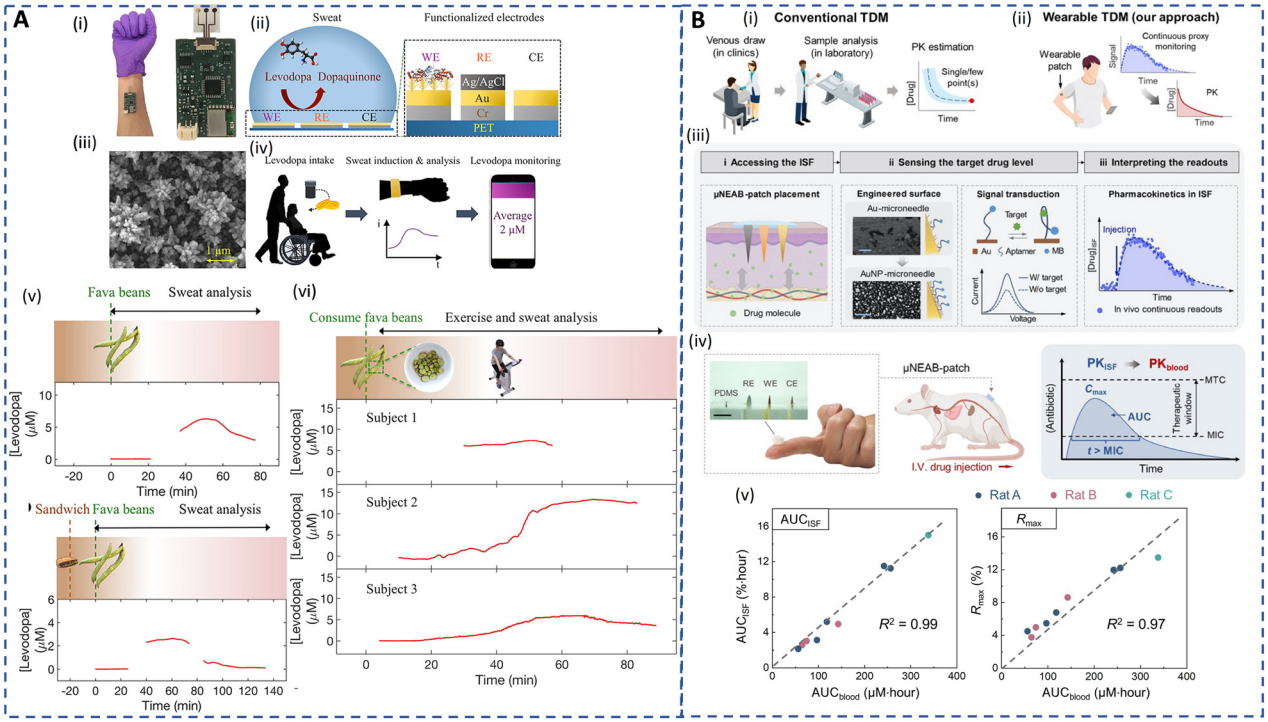

Fig. 7 Sweat- and ISF-enabled detection platforms for therapeutic drug monitoring. (A) (i) Image of sweatband sensor for L-dopa monitoring. (ii) Illustration of the sensing mechanism of the sweatband with a zoomed-in cross-sectional view of the working electrode with gold dendrites (WE), reference electrode (RE), and counter electrode (CE), respectively. (iii) Scanning electron microscope (SEM) image of the nanodendritic structures. (iv) Real-time sweat L-dopa monitoring using the sweatband after the drug intake. (v) Sweat L-dopa monitoring during iontophoresis-induced sweat on fava bean consumption without (top) and with (bottom) prior dietary intake. (vi) Sweat L-dopa monitoring during exercise-induced sweat on fava bean consumption for 3 different subjects. Reprinted with permission from Tai *et al.*[68] Copyright© 2019 American Chemical Society. (B) (i) Illustration of conventional TDM approaches involving blood sampling, laboratory tests, and single- or few-point measurement. (ii) Illustration of envisioned TDM approach involving ISF-enabled wearable patch for continuous monitoring to obtain drug pharmacokinetic characteristics. (iii) Schematic representing the working principle of the μNEAB wearable patch for continuous drug monitoring. (iv) Representation of the assembled patch applied on a rat model for *in vivo* TDM to assess the feasibility of ISF-based TDM for interpreting pharmacokinetics of antibiotics. MTC/MIC: minimally toxic/inhibitory concentrations, IV: intravenous. Reprinted with permission from Lin *et al.*[213] Copyright© 2022 AAAS.

levodopa in sweat during rest, showing that the concentration of levodopa in natural sweat typically increases with higher doses.[16] It can be noted that most of the studies for L-dopa monitoring have been based on fava or broad bean intake rather than standard pill administration for TDM. Hence, leveraging on natural sweat, Moon *et al.* developed a fingertip electrochemical sensor to analyze sweat L-dopa levels after oral tablet administration utilizing a highly permeable hydrogel to collect and transport fingertip sweat to a tyrosinase-based enzyme electrode.[83] The pharmacokinetic profile of L-dopa in sweat closely matched with the blood L-dopa concentrations with a short lag time of 10 min. Despite the progress towards personalized Parkinson's disease treatment using wearable platforms, factors like diet, hydration, metabolism rates, and drug absorption can influence the correlation between sweat and plasma levodopa levels, necessitating larger population studies for a better understanding.[16]

Acetaminophen, the most commonly prescribed over-the-counter medication, can cause liver failure, kidney dysfunction, and hepatotoxicity in case of overdose.[222,223] Sweat has been found to exhibit a strong correlation with blood concentrations of acetaminophen, making it a potential non-invasive matrix for monitoring its levels and metabolism.[215,224] Mostly, voltammetry-based sensing platforms are commonly integrated with wearables to detect electroactive drugs. However, biofouling effects and interference from endogenous electroactive substances have been reported to affect the accuracy of voltammetric sensors. To address these limitations, a wearable voltammetric sensor incorporating a Nafion-coated and hydrogen-terminated boron-doped diamond electrode (Nafion/H-BDDE) was introduced.[96] The sensor achieved accurate and reliable quantification of acetaminophen in sweat without interference from histidine, methionine, or ascorbic acid. With only minor modification, the proposed surface engineering technique can be used for quantification of various electroactive drugs both endogenous and exogenous. Recently, a wearable plasmonic sensor integrated with a microfluidic system was introduced for non-invasive acetaminophen drug monitoring in sweat.[225] The sensor utilized an Au nanosphere cone array with surface-enhanced Raman scattering (SERS) activity to detect acetaminophen selectively and sensitively at concentrations as low as 0.13

μM. This technology allows for effective monitoring of dynamic pharmacokinetics. While most studies focus on single-drug monitoring in sweat, a recent study explored a wide range of drugs with diverse physiochemical characteristics in sweat and plasma, demonstrating the potential of sweat for at-home or remote TDM.[215]

ISF, with similar composition to plasma but with a lower protein concentration, offers advantages for drug monitoring such as accurate measurement of bioavailable drug concentration, painless sampling, a simpler assay, and cost-effectiveness. However, extracting sufficient ISF for analysis is challenging. MN-integrated biosensors show promise in enabling commercially viable TDM and diagnostics.[131,220] A recent in-human study employed a potentiometric microneedle array-based biosensor for real-time monitoring of β-lactam antibiotics in ISF leveraging the pH changes upon hydrolysis of β-lactam antibiotics by β-lactamase.[226] The array, enabling detection of penicillin with a LOD of 6.8 μM, demonstrated a free drug concentration–time profile in ISF that was comparable to that of serum and a pharmacokinetic profile in ISF that closely resembled the gold standard method. This platform was also the first demonstration of an ISF-enabled automated and integrated closed-loop system to achieve individual dosing in humans. J. Wang's group developed a hollow microneedle sensing platform for continuous monitoring of levodopa, apomorphine, opioids, and nerve agents in dermal ISF.[20,227,228] The sensor was integrated within the microneedle during insertion, and it employed non-enzymatic square-wave voltammetry (SWV) and enzymatic chronoamperometry for parallel drug detection. The dual-mode L-dopa sensors showed high sensitivity, selectivity, and stability in artificial ISF. In an *ex vivo* mice skin model, the sensor exhibited distinct voltammetric and amperometric responses proportional to the drug concentration. This research group is presently conducting a clinical trial to evaluate the safety and clinical applicability of the biosensor.

DNA aptamers, which can be selected and synthesized for virtually any target, exhibit high target affinity and specificity based on precise three-dimensional complementarity, expanding the range of analytes beyond those detected by enzymes and ionophores.[35] Wu *et al.* developed an aptamer-based platform for detection of a prodrug and its metabolite at neighboring MNs on an array using ISF.[229] More recently, a MN-based electrochemical aptamer biosensing patch (μNEAB-patch) has been developed for measurement of circulating drug pharmacokinetics in ISF as depicted in Fig. 7B(i–iv).[213] The platform employed a labeled aptamer immobilized on gold nanoparticle-coated needles that underwent conformational changes for continuous detection. The relationship between the drug's circulation in blood [AUC (AUC_{blood})] and μNEAB-patch response [(AUC_{ISF}) and the maximum sensor response (R_{max})] were investigated as shown in Fig. 7B(v and vi). The μNEAB-patch successfully achieved continuous detection of the antibiotic tobramycin and vancomycin in ISF and exhibited a strong correlation with circulating drug levels in animal studies, demonstrating its potential clinical use for drug exposure prediction. Although the recent technologies are insightful, large-scale clinical studies to establish ISF-blood correlation are critical to realizing personalized and precision dosing for ambulatory care.

To summarize, Table 2 briefly discusses the various aspects of the developed sweat- and ISF-enabled sensors for non-invasive detection.

Outlook

During the COVID-19 pandemic, remote healthcare monitoring emerged as a viable alternative to face-to-face visits at hospitals, benefiting individuals, the elderly, and patients with chronic illnesses. Remote ambulatory care is valuable in enhancing the quality of care and patient engagement while expediting early detection and intervention for disease and drug management. The increasing research on biofluid-enabled sensors, particularly sweat and ISF, has shown great potential in precision medicine and preventative healthcare. As detailed in this review, there are barriers hindering their wider adoption in ambulatory care, and addressing these challenges through technological advancements remains an active area of interest. Future directions include improving accuracy and detection limits for biomarker analysis, understanding partitioning pathways and correlations with blood, conducting large-scale cohort studies, and addressing the issue of small sample volumes in sweat and ISF for accurate and reliable monitoring.

Microfluidic technology has been successful in significantly increasing sweat collection volume by utilizing a smart combination of hydrophilic and hydrophobic materials.[231] MN technology has immense potential for non-invasive monitoring in ISF at a small scale; however, its utility in comparison to conventional blood sampling presently is impaired. An ideal monitoring system must be able to sample ≥1 μL of ISF as sub-microliter volumes are prone to dilution errors and noise affecting the correlations. Researchers are actively working to address this issue and achieve meaningful biomarker analysis of clinical significance.[31,232] Another key aspect of continuous monitoring is the long-term stability of the sensing platforms, which requires robust interface strategies and stable functional materials capable of sustaining physical strain and environmental variations. Comprehensive considerations of material and structural characteristics are essential in this regard. To ensure operation stability, advancements in integrated circuit technologies can simplify circuitry and reduce device size, while self-powered nanogenerators or biofuel cells can address power consumption issues.[233,234] In addition, hybrid and efficient energy management strategies are needed to meet the demands of data transmission. Concurrent initiatives to ensure data security and the implementation of high-throughput fabrication technologies such as 3D printing

Table 2 An overview of the detection mechanism, sampling method, limit of detection and long-term operation of developed sweat- and ISF-enabled sensors for chronic disease, inflammation and therapeutic monitoring

	Analyte	Fluid	Detection mechanism	Sampling technique	Detection range	Limit of detection	Long-term operation	Ref.
Diabetes	Glucose	Sweat	Colorimetric	Microfluidic channels	4–40.4 μM	—	—	160
		Sweat	Colorimetric	Filter paper	0–0.15 mM	0.01 mM	—	162
		Sweat	Electrochemical	Rayon pad	50–200 μM	2 μM	2 hours	147
		ISF	Electrochemical	MN array (solid)	0–40 mM	0.32 mM	—	149
		ISF	Electrochemical	MN array (hydrogel)	8–22 mM	—	—	182
Diabetic ketoacidosis	β-Hydroxybutyrate (HB)	ISF	Electrochemical	MN array (hollow)	—	50 μM	6 hours	121
		Sweat	Electrochemical	Polyvinyl alcohol (PVA) gel	—	62 μM		54
Chronic kidney disease	Urea	Sweat	Colorimetric	Microfluidic channels	2–15 mM	—	—	60
		Sweat	Optical	Microfluidic channels	0–60 mmol l^{-1}	0.47 mmol l^{-1}	90 days	185
		ISF	Electrochemical	MN array (solid)	50–2500 μM	2.8 μM	—	199
	Creatinine	Sweat	Colorimetric	Microfluidic channels	9–15 mM	—	—	60
Chronic inflammation	TNF-α	Sweat	Electrochemical	Nanoporous hydrophilic membrane	1–1000 pg ml^{-1}	1 pg ml^{-1}	—	209
	IL-β	Sweat	Electrochemical	PharmChek patch	0.2–200 pg ml^{-1}	0.2 pg ml^{-1}	30 hours (on-body) 30 days (storage)	210
	IL-6	ISF	Electrochemical	MN array	0–5000 pg ml^{-1}	0.54 pg ml^{-1}	5 days	22
Therapeutic drug	L-Dopa	Sweat	Electrochemical	—	0–20 μM	1.25 μM	—	68
		Sweat	Electrochemical	Cotton pad	1–95 μM	0.45 μM	—	230
		ISF	Electrochemical	MN array (hollow)	20–300 μM	0.5 μM (non-enzymatic) 0.25 μM (enzymatic)	110 min	20

or roll-to-roll manufacturing are essential for easy translation of dermal fluid-enabled devices from laboratory- to clinical-grade products.[17,86] Age, sex, comorbidities, geographic region, medicine, lifestyle, time, and genetic variation affecting diagnostic accuracy can all have a significant impact on the clinical interpretation of biomarker data. A better understanding of the correlation between the various biomarkers and certain diseases utilizing advanced machine/deep learning (ML/DL) and artificial intelligence (AI) can assist in the clinical implementation of these biosensors.[235] Therefore, creating multifunctional systems for multiplexed detection of biomarkers integrated with AI can enable closed-loop systems with therapeutically relevant individualized outputs for smart ambulatory care.

Author contributions

H. Y. Y. Nyein conceptualized the framework and scope of the paper, co-wrote, and co-edited the review. A. Veronica led the write-up and revision of the manuscript. Y. Li assisted in gathering the content and reviewing the manuscript. Y. Li helped with the illustrations and figures. I.-M. Hsing provided feedback and co-edited the manuscript. All the authors thoroughly read the final manuscript draft and gave permission for its submission.

Conflicts of interest

There is no conflict of interest.

Acknowledgements

H. Y. Y. Nyein acknowledges the faculty start-up fund from the Hong Kong University of Science and Technology, a donation grant from the Chau Hoi Shuen Foundation, and the funding from the Research Grants Council (Grant # 26201323). I.-M. Hsing acknowledges the funding from the Research Grants Council of the Hong Kong SAR Government (Grant # C6107-20G).

References

1 F. Sana, E. M. Isselbacher, J. P. Singh, E. K. Heist, B. Pathik and A. A. Armoundas, *J. Am. Coll. Cardiol.*, 2020, **75**, 1582–1592.
2 V. Atella, A. P. Mortari, J. Kopinska, F. Belotti, F. Lapi, C. Cricelli and L. Fontana, *Aging Cell*, 2019, **18**, e12861.
3 A. Dittmar, F. Axisa, G. Delhomme and C. Gehin, in *Wearable eHealth Systems for Personalised Health Management*, IOS Press, 2004, pp. 9–35.
4 Ambulatory monitoring, **https://www.health-lighthouse.eu/ambulatory-monitoring**, (accessed May 28, 2023).

5 Noncommunicable diseases, https://www.who.int/news-room/fact-sheets/detail/noncommunicable-diseases, (accessed May 28, 2023).
6 C. O. Airhihenbuwa, T.-S. Tseng, V. D. Sutton and L. Price, *Prev. Chronic Dis.*, 2021, **18**, E33.
7 R. Reynolds, S. Dennis, I. Hasan, J. Slewa, W. Chen, D. Tian, S. Bobba and N. Zwar, *BMC Fam. Pract.*, 2018, **19**, 11.
8 Z. Qiao, S. Chen, S. Fan, Z. Xiong and C. T. Lim, *Adv. Sens. Res.*, 2023, 2200068.
9 Biomarkers Definitions Working Group, *Clin. Pharmacol. Ther.*, 2001, **69**, 89–95.
10 A. Himawan, L. K. Vora, A. D. Permana, S. Sudir, A. R. Nurdin, R. Nislawati, R. Hasyim, C. J. Scott and R. F. Donnelly, *Adv. Healthcare Mater.*, 2023, **12**, e2202066.
11 D. Sim, M. C. Brothers, J. M. Slocik, A. E. Islam, B. Maruyama, C. C. Grigsby, R. R. Naik and S. S. Kim, *Adv. Sci.*, 2022, **9**, e2104426.
12 J. Heikenfeld, A. Jajack, B. Feldman, S. W. Granger, S. Gaitonde, G. Begtrup and B. A. Katchman, *Nat. Biotechnol.*, 2019, **37**, 407–419.
13 K. Njoku, D. Chiasserini, E. R. Jones, C. E. Barr, H. O'Flynn, A. D. Whetton and E. J. Crosbie, *Front. Oncol.*, 2020, **10**, 559016.
14 I. T. Gug, M. Tertis, O. Hosu and C. Cristea, *TrAC, Trends Anal. Chem.*, 2019, **113**, 301–316.
15 H. Lee, C. Song, Y. S. Hong, M. Kim, H. R. Cho, T. Kang, K. Shin, S. H. Choi, T. Hyeon and D.-H. Kim, *Sci. Adv.*, 2017, **3**, e1601314.
16 H. Y. Y. Nyein, M. Bariya, B. Tran, C. H. Ahn, B. J. Brown, W. Ji, N. Davis and A. Javey, *Nat. Commun.*, 2021, **12**, 1823.
17 H. Y. Y. Nyein, M. Bariya, L. Kivimäki, S. Uusitalo, T. S. Liaw, E. Jansson, C. H. Ahn, J. A. Hangasky, J. Zhao, Y. Lin, T. Happonen, M. Chao, C. Liedert, Y. Zhao, L.-C. Tai, J. Hiltunen and A. Javey, *Sci. Adv.*, 2019, **5**, eaaw9906.
18 X. He, C. Fan, Y. Luo, T. Xu and X. Zhang, *npj Flexible Electron.*, 2022, **6**, 1–10.
19 Y. Cheng, X. Gong, J. Yang, G. Zheng, Y. Zheng, Y. Li, Y. Xu, G. Nie, X. Xie, M. Chen, C. Yi and L. Jiang, *Biosens. Bioelectron.*, 2022, **203**, 114026.
20 K. Y. Goud, C. Moonla, R. K. Mishra, C. Yu, R. Narayan, I. Litvan and J. Wang, *ACS Sens.*, 2019, **4**, 2196–2204.
21 M. Sang, M. Cho, S. Lim, I. S. Min, Y. Han, C. Lee, J. Shin, K. Yoon, W.-H. Yeo, T. Lee, S. M. Won, Y. Jung, Y. J. Heo and K. J. Yu, *Sci. Adv.*, 2023, **9**, eadh1765.
22 J. Xu, B. Yang, J. Kong, Y. Zhang and X. Fang, *Adv. Healthcare Mater.*, 2023, e2203133.
23 J. Min, J. Tu, C. Xu, H. Lukas, S. Shin, Y. Yang, S. A. Solomon, D. Mukasa and W. Gao, *Chem. Rev.*, 2023, **123**, 5049–5138.
24 M. Wang, Y. Yang, J. Min, Y. Song, J. Tu, D. Mukasa, C. Ye, C. Xu, N. Heflin, J. S. McCune, T. K. Hsiai, Z. Li and W. Gao, *Nat. Biomed. Eng.*, 2022, **6**, 1225–1235.
25 A. Alizadeh, A. Burns, R. Lenigk, R. Gettings, J. Ashe, A. Porter, M. McCaul, R. Barrett, D. Diamond, P. White, P. Skeath and M. Tomczak, *Lab Chip*, 2018, **18**, 2632–2641.
26 R. Das, S. Nag and P. Banerjee, *Molecules*, 2023, **28**(3), 1259.
27 M. Parrilla, I. Ortiz-Gómez, R. Cánovas, A. Salinas-Castillo, M. Cuartero and G. A. Crespo, *Anal. Chem.*, 2019, **91**, 8644–8651.
28 M. Bariya, H. Y. Y. Nyein and A. Javey, *Nat. Electron.*, 2018, **1**, 160–171.
29 J. Heikenfeld, *Electroanalysis*, 2016, **28**, 1242–1249.
30 T. Saha, R. Del Caño, E. la De Paz, S. S. Sandhu and J. Wang, *Small*, 2022, e2206064.
31 P. P. Samant, M. M. Niedzwiecki, N. Raviele, V. Tran, J. Mena-Lapaix, D. I. Walker, E. I. Felner, D. P. Jones, G. W. Miller and M. R. Prausnitz, *Sci. Transl. Med.*, 2020, **12**, eaaw0285.
32 M. Friedel, I. A. P. Thompson, G. Kasting, R. Polsky, D. Cunningham, H. T. Soh and J. Heikenfeld, *Nat. Biomed. Eng.*, 2023, DOI: 10.1038/s41551-022-00998-9.
33 D. C. Klonoff, *Diabetes Care*, 2005, **28**, 1231–1239.
34 S. Ma, J. Li, L. Pei, N. Feng and Y. Zhang, *J. Pharm. Anal.*, 2023, **13**, 111–126.
35 M. Dervisevic, M. Alba, B. Prieto-Simon and N. H. Voelcker, *Nano Today*, 2020, **30**, 100828.
36 F. Gao, C. Liu, L. Zhang, T. Liu, Z. Wang, Z. Song, H. Cai, Z. Fang, J. Chen, J. Wang, M. Han, J. Wang, K. Lin, R. Wang, M. Li, Q. Mei, X. Ma, S. Liang, G. Gou and N. Xue, *Microsyst. Nanoeng.*, 2023, **9**, 1.
37 D. S. Yang, R. Ghaffari and J. A. Rogers, *Science*, 2023, **379**, 760–761.
38 K. Wilke, A. Martin, L. Terstegen and S. S. Biel, *Int. J. Cosmet. Sci.*, 2007, **29**, 169–179.
39 A. J. Hendricks, A. R. Vaughn, A. K. Clark, G. Yosipovitch and V. Y. Shi, *J. Dermatol. Sci.*, 2018, **89**, 105–111.
40 J. Xu, Y. Fang and J. Chen, *Biosensors*, 2021, **11**(8), 245.
41 E. J. M. Moonen, J. R. Haakma, E. Peri, E. Pelssers, M. Mischi and J. M. J. den Toonder, *View*, 2020, **1**, 20200077.
42 S. Jadoon, S. Karim, M. R. Akram, A. Kalsoom Khan, M. A. Zia, A. R. Siddiqi and G. Murtaza, *Int. J. Anal. Chem.*, 2015, **2015**, 164974.
43 E. Morales, P. Cravedi and J. Manrique, *Front. Med.*, 2021, **8**, 653634.
44 Z. Sonner, E. Wilder, J. Heikenfeld, G. Kasting, F. Beyette, D. Swaile, F. Sherman, J. Joyce, J. Hagen, N. Kelley-Loughnane and R. Naik, *Biomicrofluidics*, 2015, **9**, 031301.
45 F. T. S. M. Ferreira, R. B. R. Mesquita and A. O. S. S. Rangel, *Microchem. J.*, 2023, **193**, 109102.
46 M. Bhogadia, M. Edgar, K. Hunwin, G. Page and M. Grootveld, *Metabolites*, 2023, **13**(7), 792.
47 P. P. Ricci and O. J. Gregory, *Sci. Rep.*, 2021, **11**, 7185.
48 D. Czarnowski, J. Górski, J. Jóźwiuk and A. Boroń-Kaczmarska, *Eur. J. Appl. Physiol. Occup. Physiol.*, 1992, **65**, 135–137.
49 A. Tricoli and G. Neri, *Sensors*, 2018, **18**(4), 942.
50 B. Zhu, X. Li, L. Zhou and B. Su, *Electroanalysis*, 2022, **34**, 237–245.

51 I. Lee, D. Probst, D. Klonoff and K. Sode, *Biosens. Bioelectron.*, 2021, **181**, 113054.
52 J. Moyer, D. Wilson, I. Finkelshtein, B. Wong and R. Potts, *Diabetes Technol. Ther.*, 2012, **14**, 398–402.
53 T. D. La Count, A. Jajack, J. Heikenfeld and G. B. Kasting, *J. Pharm. Sci.*, 2019, **108**, 364–371.
54 J.-M. Moon, R. Del Caño, C. Moonla, K. Sakdaphetsiri, T. Saha, L. F. Mendes, L. Yin, A.-Y. Chang, S. Seker and J. Wang, *ACS Sens.*, 2022, **7**, 3973–3981.
55 D. Pandya, A. K. Nagrajappa and K. S. Ravi, *J. Clin. Diagn. Res.*, 2016, **10**, ZC58–ZC62.
56 Y. Y. Al-Tamer, E. A. Hadi and I. I. Al-Badrani, *Urol. Res.*, 1997, **25**, 337–340.
57 R. W. Keller, J. L. Bailey, Y. Wang, J. D. Klein and J. M. Sands, *Physiol. Rep.*, 2016, **4**(11), e12825.
58 C.-T. Huang, M.-L. Chen, L.-L. Huang and I.-F. Mao, *Chin. J. Physiol.*, 2002, **45**, 109–115.
59 Y. Yang, Y. Song, X. Bo, J. Min, O. S. Pak, L. Zhu, M. Wang, J. Tu, A. Kogan, H. Zhang, T. K. Hsiai, Z. Li and W. Gao, *Nat. Biotechnol.*, 2020, **38**, 217–224.
60 Y. Zhang, H. Guo, S. B. Kim, Y. Wu, D. Ostojich, S. H. Park, X. Wang, Z. Weng, R. Li, A. J. Bandodkar, Y. Sekine, J. Choi, S. Xu, S. Quaggin, R. Ghaffari and J. A. Rogers, *Lab Chip*, 2019, **19**, 1545–1555.
61 C. Liu, D. Chu, K. Kalantar-Zadeh, J. George, H. A. Young and G. Liu, *Adv. Sci.*, 2021, **8**, e2004433.
62 B. Jagannath, K.-C. Lin, M. Pali, D. Sankhala, S. Muthukumar and S. Prasad, *Bioeng. Transl. Med.*, 2021, **6**, e10220.
63 A. Marques-Deak, G. Cizza, F. Eskandari, S. Torvik, I. C. Christie, E. M. Sternberg, T. M. Phillips and Premenopausal, Osteoporosis Women, Alendronate, Depression Study Group, *J. Immunol. Methods*, 2006, **315**, 99–109.
64 M. D. Hladek, S. L. Szanton, Y.-E. Cho, C. Lai, C. Sacko, L. Roberts and J. Gill, *J. Immunol. Methods*, 2018, **454**, 1–5.
65 J. S. Kang and M. H. Lee, *Korean J. Intern. Med.*, 2009, **24**, 1–10.
66 N. Brasier, A. Widmer, M. Osthoff, M. Mutke, F. De Ieso, P. Brasier-Lutz, L. Wolfe, V. Aithal, C. D. Broeckling, J. Prenni and J. Eckstein, *Front. Med.*, 2020, **7**, 476.
67 N. Brasier, A. Widmer, M. Osthoff, M. Mutke, F. De Ieso, P. Brasier-Lutz, K. Brown, L. Yao, C. D. Broeckling, J. Prenni and J. Eckstein, *Digit. Biomark.*, 2021, **5**, 24–28.
68 L.-C. Tai, T. S. Liaw, Y. Lin, H. Y. Y. Nyein, M. Bariya, W. Ji, M. Hettick, C. Zhao, J. Zhao, L. Hou, Z. Yuan, Z. Fan and A. Javey, *Nano Lett.*, 2019, **19**, 6346–6351.
69 M. Tsunoda, M. Hirayama, T. Tsuda and K. Ohno, *Clin. Chim. Acta*, 2015, **442**, 52–55.
70 W. Gao, S. Emaminejad, H. Y. Y. Nyein, S. Challa, K. Chen, A. Peck, H. M. Fahad, H. Ota, H. Shiraki, D. Kiriya, D.-H. Lien, G. A. Brooks, R. W. Davis and A. Javey, *Nature*, 2016, **529**, 509–514.
71 S. Imani, A. J. Bandodkar, A. M. V. Mohan, R. Kumar, S. Yu, J. Wang and P. P. Mercier, *Nat. Commun.*, 2016, **7**, 11650.
72 L. B. Baker, *Sports Med.*, 2017, **47**, 111–128.
73 M. J. Buono and N. T. Sjoholm, *J. Appl. Physiol.*, 1988, **65**, 811–814.
74 J. Kim, I. Jeerapan, S. Imani, T. N. Cho, A. Bandodkar, S. Cinti, P. P. Mercier and J. Wang, *ACS Sens.*, 2016, **1**, 1011–1019.
75 S. Emaminejad, W. Gao, E. Wu, Z. A. Davies, H. Y. Y. Nyein, S. Challa, S. P. Ryan, H. M. Fahad, K. Chen, Z. Shahpar, S. Talebi, C. Milla, A. Javey and R. W. Davis, *Proc. Natl. Acad. Sci. U. S. A.*, 2017, **114**, 4625–4630.
76 Z. Sonner, E. Wilder, T. Gaillard, G. Kasting and J. Heikenfeld, *Lab Chip*, 2017, **17**, 2550–2560.
77 P. Simmers, S. K. Li, G. Kasting and J. Heikenfeld, *J. Dermatol. Sci.*, 2018, **89**, 40–51.
78 J. Brunmair, M. Gotsmy, L. Niederstaetter, B. Neuditschko, A. Bileck, A. Slany, M. L. Feuerstein, C. Langbauer, L. Janker, J. Zanghellini, S. M. Meier-Menches and C. Gerner, *Nat. Commun.*, 2021, **12**, 5993.
79 H. Yu and J. Sun, *Nanotechnol. Precis. Eng.*, 2020, **3**, 126–140.
80 J. R. Sempionatto, J.-M. Moon and J. Wang, *ACS Sens.*, 2021, **6**, 1875–1883.
81 S. Lin, B. Wang, Y. Zhao, R. Shih, X. Cheng, W. Yu, H. Hojaiji, H. Lin, C. Hoffman, D. Ly, J. Tan, Y. Chen, D. Di Carlo, C. Milla and S. Emaminejad, *ACS Sens.*, 2020, **5**, 93–102.
82 K. Nagamine, T. Mano, A. Nomura, Y. Ichimura, R. Izawa, H. Furusawa, H. Matsui, D. Kumaki and S. Tokito, *Sci. Rep.*, 2019, **9**, 10102.
83 J.-M. Moon, H. Teymourian, E. De la Paz, J. R. Sempionatto, K. Mahato, T. Sonsa-Ard, N. Huang, K. Longardner, I. Litvan and J. Wang, *Angew. Chem.*, 2021, **60**, 19074–19078.
84 A. Martín, J. Kim, J. F. Kurniawan, J. R. Sempionatto, J. R. Moreto, G. Tang, A. S. Campbell, A. Shin, M. Y. Lee, X. Liu and J. Wang, *ACS Sens.*, 2017, **2**, 1860–1868.
85 C.-C. Tseng, C.-T. Kung, R.-F. Chen, M.-H. Tsai, H.-R. Chao, Y.-N. Wang and L.-M. Fu, *Sens. Actuators, B*, 2021, **342**, 130078.
86 C.-H. Wu, H. J. H. Ma, P. Baessler, R. K. Balanay and T. R. Ray, *Sci. Adv.*, 2023, **9**, eadg4272.
87 D. Liu, Z. Liu, S. Feng, Z. Gao, R. Chen, G. Cai and S. Bian, *Biosensors*, 2023, **13**(2), 157.
88 H. Y. Y. Nyein, L.-C. Tai, Q. P. Ngo, M. Chao, G. B. Zhang, W. Gao, M. Bariya, J. Bullock, H. Kim, H. M. Fahad and A. Javey, *ACS Sens.*, 2018, **3**, 944–952.
89 J. R. Sempionatto, J. A. Lasalde-Ramírez, K. Mahato, J. Wang and W. Gao, *Nat. Rev. Chem.*, 2022, **6**, 899–915.
90 D. Kukkar, D. Zhang, B. H. Jeon and K.-H. Kim, *TrAC, Trends Anal. Chem.*, 2022, **150**, 116570.
91 X. Zhang, Y. Xia, Y. Liu, S. M. Mugo and Q. Zhang, *Anal. Chem.*, 2022, **94**, 993–1002.
92 D. D. H. Franke and M. A. Connelly, in *Contemporary Practice in Clinical Chemistry*, ed. W. Clarke and M. A. Marzinke, Academic Press, 4th edn, 2020, pp. 187–200.
93 X. Yuan, O. Ouaskioud, X. Yin, C. Li, P. Ma, Y. Yang, P.-F. Yang, L. Xie and L. Ren, *Micromachines*, 2023, **14**(7), 1452.

94 Y.-J. Chen, Y.-P. Hsu, Y.-L. Tain, N.-S. Li, H.-H. Pang, S.-W. Kuo and H.-W. Yang, *Biosens. Bioelectron.*, 2022, **208**, 114234.
95 H. Teymourian, M. Parrilla, J. R. Sempionatto, N. F. Montiel, A. Barfidokht, R. Van Echelpoel, K. De Wael and J. Wang, *ACS Sens.*, 2020, **5**, 2679–2700.
96 S. Lin, W. Yu, B. Wang, Y. Zhao, K. En, J. Zhu, X. Cheng, C. Zhou, H. Lin, Z. Wang, H. Hojaiji, C. Yeung, C. Milla, R. W. Davis and S. Emaminejad, *Proc. Natl. Acad. Sci. U. S. A.*, 2020, **117**, 19017–19025.
97 J. Choi, D. Kang, S. Han, S. B. Kim and J. A. Rogers, *Adv. Healthcare Mater.*, 2017, **6**(5), 1601355.
98 J. Choi, Y. Xue, W. Xia, T. R. Ray, J. T. Reeder, A. J. Bandodkar, D. Kang, S. Xu, Y. Huang and J. A. Rogers, *Lab Chip*, 2017, **17**, 2572–2580.
99 S. B. Kim, Y. Zhang, S. M. Won, A. J. Bandodkar, Y. Sekine, Y. Xue, J. Koo, S. W. Harshman, J. A. Martin, J. M. Park, T. R. Ray, K. E. Crawford, K.-T. Lee, J. Choi, R. L. Pitsch, C. C. Grigsby, A. J. Strang, Y.-Y. Chen, S. Xu, J. Kim, A. Koh, J. S. Ha, Y. Huang, S. W. Kim and J. A. Rogers, *Small*, 2018, **14**, e1703334.
100 T. Trantidou, Y. Elani, E. Parsons and O. Ces, *Microsyst. Nanoeng.*, 2017, **3**, 16091.
101 T. Shay, M. D. Dickey and O. D. Velev, *Lab Chip*, 2017, **17**, 710–716.
102 C. Nie, A. J. H. Frijns, R. Mandamparambil and J. M. J. den Toonder, *Biomed. Microdevices*, 2015, **17**, 47.
103 X.-M. Chen, Y.-J. Li, D. Han, H.-C. Zhu, C.-D. Xue, H.-C. Chui, T. Cao and K.-R. Qin, *Micromachines*, 2019, **10**(7), 457.
104 C. Liu, T. Xu, D. Wang and X. Zhang, *Talanta*, 2020, **212**, 120801.
105 X. He, T. Xu, Z. Gu, W. Gao, L.-P. Xu, T. Pan and X. Zhang, *Anal. Chem.*, 2019, **91**, 4296–4300.
106 P. Xi, X. He, C. Fan, Q. Zhu, Z. Li, Y. Yang, X. Du and T. Xu, *Talanta*, 2023, **259**, 124507.
107 X. He, S. Yang, Q. Pei, Y. Song, C. Liu, T. Xu and X. Zhang, *ACS Sens.*, 2020, **5**, 1548–1554.
108 X. Hong, H. Wu, C. Wang, X. Zhang, C. Wei, Z. Xu, D. Chen and X. Huang, *ACS Appl. Mater. Interfaces*, 2022, **14**, 9644–9654.
109 W. F. Brechue and H. T. Hammel, *Comp. Exerc. Physiol.*, 2010, **7**, 153–171.
110 R. Ibrahim, J. M. Nitsche and G. B. Kasting, *J. Pharm. Sci.*, 2012, **101**, 2094–2108.
111 S. Ono, G. Egawa and K. Kabashima, *Inflammation Regener.*, 2017, **37**, 11.
112 M. Gilányi, C. Ikrényi, J. Fekete, K. Ikrényi and A. G. Kovách, *Am. J. Physiol.*, 1988, **255**, F513–F519.
113 M. Parrilla, M. Cuartero, S. P. Sánchez, M. Rajabi, N. Roxhed, F. Niklaus and G. A. Crespo, *Anal. Chem.*, 2019, **91**, 1578–1586.
114 S. N. Thennadil, J. L. Rennert, B. J. Wenzel, K. H. Hazen, T. L. Ruchti and M. B. Block, *Diabetes Technol. Ther.*, 2001, **3**, 357–365.
115 F. J. Service, P. C. O'Brien, S. D. Wise, S. Ness and S. M. LeBlanc, *Diabetes Care*, 1997, **20**, 1426–1429.
116 M. Sinha, K. M. McKeon, S. Parker, L. G. Goergen, H. Zheng, F. H. El-Khatib and S. J. Russell, *J. Diabetes Sci. Technol.*, 2017, **11**, 1132–1137.
117 D. B. Keenan, J. J. Mastrototaro, G. Voskanyan and G. M. Steil, *J. Diabetes Sci. Technol.*, 2009, **3**, 1207–1214.
118 G. Schmelzeisen-Redeker, M. Schoemaker, H. Kirchsteiger, G. Freckmann, L. Heinemann and L. Del Re, *J. Diabetes Sci. Technol.*, 2015, **9**, 1006–1015.
119 T. Shi, Y. Zhang and L. Lu, *Biotechnol. Biotechnol. Equip.*, 2018, **32**, 1047–1052.
120 C. R. Barnett and Y. A. Barnett, in *Encyclopedia of Food Sciences and Nutrition*, ed. B. Caballero, Academic Press, Oxford, 2nd edn, 2003, pp. 3421–3425.
121 H. Teymourian, C. Moonla, F. Tehrani, E. Vargas, R. Aghavali, A. Barfidokht, T. Tangkuaram, P. P. Mercier, E. Dassau and J. Wang, *Anal. Chem.*, 2020, **92**, 2291–2300.
122 A. J. Taylor and P. Vadgama, *Ann. Clin. Biochem.*, 1992, **29**(Pt 3), 245–264.
123 A. J. Bandodkar, W. Jia, C. Yardımcı, X. Wang, J. Ramirez and J. Wang, *Anal. Chem.*, 2015, **87**, 394–398.
124 M. Zheng, Z. Wang, H. Chang, L. Wang, S. W. T. Chew, D. C. S. Lio, M. Cui, L. Liu, B. C. K. Tee and C. Xu, *Adv. Healthcare Mater.*, 2020, **9**, e1901683.
125 L. Ebah, P. Brenchley, B. Coupes and S. Mitra, *Blood Purif.*, 2011, **32**, 96–103.
126 L. M. Ebah, Doctor of Philosophy in the Faculty of Medical and Human Sciences, *PhD*, University of Manchester, 2012.
127 J. A. Stenken and A. J. Poschenrieder, *Anal. Chim. Acta*, 2015, **853**, 95–115.
128 M. Mussap and M. Plebani, *Crit. Rev. Clin. Lab. Sci.*, 2004, **41**, 467–550.
129 T. Nedrebø, R. K. Reed, R. Jonsson, A. Berg and H. Wiig, *J. Physiol.*, 2004, **556**, 193–202.
130 Z. Wang, J. Luan, A. Seth, L. Liu, M. You, P. Gupta, P. Rathi, Y. Wang, S. Cao, Q. Jiang, X. Zhang, R. Gupta, Q. Zhou, J. J. Morrissey, E. L. Scheller, J. S. Rudra and S. Singamaneni, *Nat. Biomed. Eng.*, 2021, **5**, 64–76.
131 T. K. L. Kiang, S. A. Ranamukhaarachchi and M. H. H. Ensom, *Pharmaceutics*, 2017, **9**(4), 43.
132 T. K. L. Kiang, U. O. Häfeli and M. H. H. Ensom, *Clin. Pharmacokinet.*, 2014, **53**, 695–730.
133 Y. Ito, Y. Inagaki, S. Kobuchi, K. Takada and T. Sakaeda, *Int. J. Med. Sci.*, 2016, **13**, 271–276.
134 S. Park, Y. J. Kim, E. Kostal, V. Matylitskaya, S. Partel and W. Ryu, *Biosens. Bioelectron.*, 2023, **220**, 114912.
135 H. Haslene-Hox, E. Oveland, K. C. Berg, O. Kolmannskog, K. Woie, H. B. Salvesen, O. Tenstad and H. Wiig, *PLoS One*, 2011, **6**, e19217.
136 J. K. Heltne, P. Husby, M. E. Koller and T. Lund, *Lab. Anim.*, 1998, **32**, 439–445.
137 Y. Liu, X. Luo, Q. Yu, L. Ye, L. Yang and Y. Cui, *Sens. Actuators Rep.*, 2022, **4**, 100113.
138 H. Zheng, Z. Pu, H. Wu, C. Li, X. Zhang and D. Li, *Biosens. Bioelectron.*, 2023, **223**, 115036.

139 J. J. García-Guzmán, C. Pérez-Ràfols, M. Cuartero and G. A. Crespo, *TrAC, Trends Anal. Chem.*, 2021, **135**, 116148.
140 F. K. Aldawood, A. Andar and S. Desai, *Polymers*, 2021, **13**(16), 2815.
141 T. Wu, X. You and Z. Chen, *Sensors*, 2022, **22**(11), 4253.
142 K. Yi, Y. Wang, K. Shi, J. Chi, J. Lyu and Y. Zhao, *Biosens. Bioelectron.*, 2021, **190**, 113404.
143 R. He, Y. Niu, Z. Li, A. Li, H. Yang, F. Xu and F. Li, *Adv. Healthcare Mater.*, 2020, **9**, e1901201.
144 A. Jina, M. J. Tierney, J. A. Tamada, S. McGill, S. Desai, B. Chua, A. Chang and M. Christiansen, *J. Diabetes Sci. Technol.*, 2014, **8**, 483–487.
145 J. G. Turner, L. R. White, P. Estrela and H. S. Leese, *Macromol. Biosci.*, 2021, **21**, e2000307.
146 H. Sun, P. Saeedi, S. Karuranga, M. Pinkepank, K. Ogurtsova, B. B. Duncan, C. Stein, A. Basit, J. C. N. Chan, J. C. Mbanya, M. E. Pavkov, A. Ramachandaran, S. H. Wild, S. James, W. H. Herman, P. Zhang, C. Bommer, S. Kuo, E. J. Boyko and D. J. Magliano, *Diabetes Res. Clin. Pract.*, 2022, **183**, 109119.
147 J. Zhao, Y. Lin, J. Wu, H. Y. Y. Nyein, M. Bariya, L.-C. Tai, M. Chao, W. Ji, G. Zhang, Z. Fan and A. Javey, *ACS Sens.*, 2019, **4**, 1925–1933.
148 L. Lipani, B. G. R. Dupont, F. Doungmene, F. Marken, R. M. Tyrrell, R. H. Guy and A. Ilie, *Nat. Nanotechnol.*, 2018, **13**, 504–511.
149 F. Tehrani, H. Teymourian, B. Wuerstle, J. Kavner, R. Patel, A. Furmidge, R. Aghavali, H. Hosseini-Toudeshki, C. Brown, F. Zhang, K. Mahato, Z. Li, A. Barfidokht, L. Yin, P. Warren, N. Huang, Z. Patel, P. P. Mercier and J. Wang, *Nat. Biomed. Eng.*, 2022, **6**, 1214–1224.
150 S. Liu, Z. Shen, L. Deng and G. Liu, *Biosens. Bioelectron.*, 2022, **209**, 114251.
151 K. Lian, H. Feng, S. Liu, K. Wang, Q. Liu, L. Deng, G. Wang, Y. Chen and G. Liu, *Biosens. Bioelectron.*, 2022, **203**, 114029.
152 A. Waghmare, F. S. Parizi, J. Hoffman, Y. Wang, M. Thompson and S. Patel, *Proc. ACM Interact. Mob. Wearable Ubiquitous Technol.*, 2023, **7**, 1–20.
153 A. Y. Alhaddad, H. Aly, H. Gad, A. Al-Ali, K. K. Sadasivuni, J.-J. Cabibihan and R. A. Malik, *Front. Bioeng. Biotechnol.*, 2022, **10**, 876672.
154 W. V. Gonzales, A. T. Mobashsher and A. Abbosh, *Sensors*, 2019, **19**(4), 800.
155 E. V. Karpova, E. V. Shcherbacheva, A. A. Galushin, D. V. Vokhmyanina, E. E. Karyakina and A. A. Karyakin, *Anal. Chem.*, 2019, **91**, 3778–3783.
156 H. Zafar, A. Channa, V. Jeoti and G. M. Stojanović, *Sensors*, 2022, **22**(2), 638.
157 J. Kim, A. S. Campbell and J. Wang, *Talanta*, 2018, **177**, 163–170.
158 L. Tang, S. J. Chang, C.-J. Chen and J.-T. Liu, *Sensors*, 2020, **20**(23), 6925.
159 J. Zhang, J. Xu, J. Lim, J. K. Nolan, H. Lee and C. H. Lee, *Adv. Healthcare Mater.*, 2021, **10**, e2100194.
160 J. Choi, A. J. Bandodkar, J. T. Reeder, T. R. Ray, A. Turnquist, S. B. Kim, N. Nyberg, A. Hourlier-Fargette, J. B. Model, A. J. Aranyosi, S. Xu, R. Ghaffari and J. A. Rogers, *ACS Sens.*, 2019, **4**, 379–388.
161 Ö. Kap, V. Kılıç, J. G. Hardy and N. Horzum, *Analyst*, 2021, **146**, 2784–2806.
162 A. Vaquer, E. Barón and R. de la Rica, *Analyst*, 2021, **146**, 3273–3279.
163 P.-H. Lin, S.-C. Sheu, C.-W. Chen, S.-C. Huang and B.-R. Li, *Talanta*, 2022, **241**, 123187.
164 S. Y. Oh, S. Y. Hong, Y. R. Jeong, J. Yun, H. Park, S. W. Jin, G. Lee, J. H. Oh, H. Lee, S.-S. Lee and J. S. Ha, *ACS Appl. Mater. Interfaces*, 2018, **10**, 13729–13740.
165 Q. Cao, B. Liang, T. Tu, J. Wei, L. Fang and X. Ye, *RSC Adv.*, 2019, **9**, 5674–5681.
166 D. Sankhala, A. U. Sardesai, M. Pali, K.-C. Lin, B. Jagannath, S. Muthukumar and S. Prasad, *Sci. Rep.*, 2022, **12**, 2442.
167 S. M. Khor, J. Choi, P. Won and S. H. Ko, *Nanomaterials*, 2022, **12**(2), 221.
168 M. M. Alam and M. M. R. Howlader, *Sens. Bio-Sens. Res.*, 2021, **34**, 100453.
169 T. Meng, H. Jia, H. Ye, T. Zeng, X. Yang, H. Wang and Y. Zhang, *J. Colloid Interface Sci.*, 2020, **560**, 1–10.
170 Y. Zhang, D. Zheng, S. Liu, S. Qin, X. Sun, Z. Wang, C. Qin, Y. Li and J. Zhou, *Appl. Surf. Sci.*, 2021, **552**, 149529.
171 X. Strakosas, J. Selberg, P. Pansodtee, N. Yonas, P. Manapongpun, M. Teodorescu and M. Rolandi, *Sci. Rep.*, 2019, **9**, 10844.
172 Q.-F. Li, X. Chen, H. Wang, M. Liu and H.-L. Peng, *ACS Appl. Mater. Interfaces*, 2023, **15**, 13290–13298.
173 K. Rebrin and G. M. Steil, *Diabetes Technol. Ther.*, 2000, **2**, 461–472.
174 N. J. Caplin, P. O'Leary, M. Bulsara, E. A. Davis and T. W. Jones, *Diabetic Med.*, 2003, **20**, 238–241.
175 B. M. Jensen, P. Bjerring, J. S. Christiansen and H. Orskov, *Scand. J. Clin. Lab. Invest.*, 1995, **55**, 427–432.
176 J. B. Welsh, X. Zhang, S. A. Puhr, T. K. Johnson, T. C. Walker, A. K. Balo and D. Price, *J. Diabetes Sci. Technol.*, 2019, **13**, 254–258.
177 T. Bailey, B. W. Bode, M. P. Christiansen, L. J. Klaff and S. Alva, *Diabetes Technol. Ther.*, 2015, **17**, 787–794.
178 N. N. Chan and S. J. Hurel, *Pract. Diabetes Int.*, 2002, **19**, 97–100.
179 T. Nunnold, S. R. Colberg, M. T. Herriott and C. T. Somma, *Diabetes Technol. Ther.*, 2004, **6**, 454–462.
180 H. Teymourian, A. Barfidokht and J. Wang, *Chem. Soc. Rev.*, 2020, **49**, 7671–7709.
181 S. Sharma, A. El-Laboudi, M. Reddy, N. Jugnee, S. Sivasubramaniyam, M. El Sharkawy, P. Georgiou, D. Johnston, N. Oliver and A. E. G. Cass, *Anal. Methods*, 2018, **10**, 2088–2095.
182 Y. Wang, H. Liu, X. Yang, Z. Shi, J. Li, L. Xue, S. Liu and Y. Lei, *Smart Mater. Med.*, 2023, **4**, 69–77.
183 K. K. Dhatariya, N. S. Glaser, E. Codner and G. E. Umpierrez, *Nat. Rev. Dis. Primers*, 2020, **6**, 40.

184 R. Del Caño, T. Saha, C. Moonla, E. De la Paz and J. Wang, *TrAC, Trends Anal. Chem.*, 2023, **159**, 116938.
185 A. Golparvar, J. Kim, A. Boukhayma, D. Briand and S. Carrara, *Sens. Actuators, B*, 2023, **387**, 133814.
186 D. F. S. Fonseca, P. C. Costa, I. F. Almeida, P. Dias-Pereira, I. Correia-Sá, V. Bastos, H. Oliveira, C. Vilela, A. J. D. Silvestre and C. S. R. Freire, *Macromol. Biosci.*, 2020, **20**, e2000195.
187 P. Romagnani, G. Remuzzi, R. Glassock, A. Levin, K. J. Jager, M. Tonelli, Z. Massy, C. Wanner and H.-J. Anders, *Nat. Rev. Dis. Primers*, 2017, **3**, 17088.
188 K. Kalantar-Zadeh, T. H. Jafar, D. Nitsch, B. L. Neuen and V. Perkovic, *Lancet*, 2021, **398**, 786–802.
189 A. S. Levey, J. P. Bosch, J. B. Lewis, T. Greene, N. Rogers and D. Roth, *Ann. Intern. Med.*, 1999, **130**, 461–470.
190 A. O. Hosten, *BUN and Creatinine*, Butterworths, 1990.
191 Urea and creatinine concentration, the urea : creatinine ratio, **https://acutecaretesting.org/en/articles/urea-and-creatinine-concentration-the-urea-creatinine-ratio**, (accessed June 5, 2023).
192 V. R. Biljak, L. Honović, J. Matica, B. Krešić and S. Š. Vojak, *Biochem. Med.*, 2017, **27**, 153–176.
193 Y.-L. Liu, R. Liu, Y. Qin, Q.-F. Qiu, Z. Chen, S.-B. Cheng and W.-H. Huang, *Anal. Chem.*, 2018, **90**, 13081–13087.
194 S. Salatiello, M. Spinelli, C. Cassiano, A. Amoresano, F. Marini and S. Cinti, *Anal. Chim. Acta*, 2022, **1210**, 339882.
195 M. Z. Uddin, W. Khaksar and J. Torresen, *Sensors*, 2018, **18**(7), 2027.
196 T. Zhao, Y. Fu, C. Sun, X. Zhao, C. Jiao, A. Du, Q. Wang, Y. Mao and B. Liu, *Biosens. Bioelectron.*, 2022, **205**, 114115.
197 L. M. Ebah, I. Read, A. Sayce, J. Morgan, C. Chaloner, P. Brenchley and S. Mitra, *Eur. J. Clin. Invest.*, 2012, **42**, 840–847.
198 E. Varadharaj and N. Jampana, *J. Electrochem. Soc.*, 2016, **163**, B340–B347.
199 M. Senel, M. Dervisevic and N. H. Voelcker, *Mater. Lett.*, 2019, **243**, 50–53.
200 A. Grubb, U. Nyman, J. Björk, V. Lindström, B. Rippe, G. Sterner and A. Christensson, *Clin. Chem.*, 2005, **51**, 1420–1431.
201 A. Grubb, *eJIFCC*, 2017, **28**, 268–276.
202 R. Kumaresan and P. Giri, *Oman Med. J.*, 2011, **26**, 421–425.
203 I. Badillo-Ramírez, Y. J. P. Carreón, C. Rodríguez-Almazán, C. M. Medina-Durán, S. R. Islas and J. M. Saniger, *Biosensors*, 2022, **12**(4), 244.
204 L. Chen, H. Deng, H. Cui, J. Fang, Z. Zuo, J. Deng, Y. Li, X. Wang and L. Zhao, *Oncotarget*, 2018, **9**, 7204–7218.
205 K. B. Megha, X. Joseph, V. Akhil and P. V. Mohanan, *Phytomedicine*, 2021, **91**, 153712.
206 L. Koelman, O. Pivovarova-Ramich, A. F. H. Pfeiffer, T. Grune and K. Aleksandrova, *Immun. Ageing*, 2019, **16**, 11.
207 E. L. Chiswick, E. Duffy, B. Japp and D. Remick, *Methods Mol. Biol.*, 2012, **844**, 15–30.
208 C. Fitting, M. Parlato, M. Adib-Conquy, N. Memain, F. Philippart, B. Misset, M. Monchi, J.-M. Cavaillon and C. Adrie, *PLoS One*, 2012, **7**, e38916.
209 S. Upasham, A. Bhide, K.-C. Lin and S. Prasad, *Future Sci. OA*, 2020, **7**, FSO628.
210 B. Jagannath, K.-C. Lin, M. Pali, D. Sankhala, S. Muthukumar and S. Prasad, *Inflammatory Bowel Dis.*, 2020, **26**, 1533–1542.
211 A. Kothari, B. Jagannath, S. Muthukumar and S. Prasad, *Biosens. Bioelectron.: X*, 2022, **10**, 100122.
212 D. Oliveira, B. P. Correia, S. Sharma and F. T. C. Moreira, *ACS Omega*, 2022, **7**, 39039–39044.
213 S. Lin, X. Cheng, J. Zhu, B. Wang, D. Jelinek, Y. Zhao, T.-Y. Wu, A. Horrillo, J. Tan, J. Yeung, W. Yan, S. Forman, H. A. Coller, C. Milla and S. Emaminejad, *Sci. Adv.*, 2022, **8**, eabq4539.
214 M. A. Goode and J. G. Gums, *Ann. Pharmacother.*, 1993, **27**, 502–505.
215 T. Ruwe, E. White, A. S. Zebertavage, D. Runnoe, D. Fay, H. Daumeyer, T. S. Tracy, K. F. Uchtman, G. Begtrup, Y. Yuan, J. Heikenfeld and W. A. Buggele, *Ther. Drug Monit.*, 2023, DOI: **10.1097/FTD.0000000000001110**.
216 J. A. Roberts, W. W. Hope and J. Lipman, *Int. J. Antimicrob. Agents*, 2010, **35**, 419–420.
217 M. H. Ensom, G. A. Davis, C. D. Cropp and R. J. Ensom, *Clin. Pharmacokinet.*, 1998, **34**, 265–279.
218 K. S. R. Raju, I. Taneja, S. P. Singh and Wahajuddin, *Biomed. Chromatogr.*, 2013, **27**, 1354–1366.
219 E. Marchei, M. Farrè, M. Pellegrini, O. García-Algar, O. Vall, R. Pacifici and S. Pichini, *Forensic Sci. Int.*, 2010, **196**, 59–63.
220 H. C. Ates, J. A. Roberts, J. Lipman, A. E. G. Cass, G. A. Urban and C. Dincer, *Trends Biotechnol.*, 2020, **38**, 1262–1277.
221 E. De Rycke, C. Stove, P. Dubruel, S. De Saeger and N. Beloglazova, *Biosens. Bioelectron.*, 2020, **169**, 112579.
222 E. M. Lancaster, J. R. Hiatt and A. Zarrinpar, *Arch. Toxicol.*, 2015, **89**, 193–199.
223 E. Roberts, V. D. Nunes, S. Buckner, S. Latchem, M. Constanti, P. Miller, M. Doherty, W. Zhang, F. Birrell, M. Porcheret, K. Dziedzic, I. Bernstein, E. Wise and P. G. Conaghan, *Ann. Rheum. Dis.*, 2016, **75**, 552–559.
224 S. Lin, B. Wang, W. Yu, K. Castillo, C. Hoffman, X. Cheng, Y. Zhao, Y. Gao, Z. Wang, H. Lin, H. Hojaiji, J. Tan and S. Emaminejad, *ACS Sens.*, 2020, **5**, 265–273.
225 J. Xiao, J. Wang, Y. Luo, T. Xu and X. Zhang, *ACS Sens.*, 2023, **8**, 1766–1773.
226 T. M. Rawson, S. A. N. Gowers, D. M. E. Freeman, R. C. Wilson, S. Sharma, M. Gilchrist, A. MacGowan, A. Lovering, M. Bayliss, M. Kyriakides, P. Georgiou, A. E. G. Cass, D. O'Hare and A. H. Holmes, *Lancet Digital Health*, 2019, **1**, e335–e343.
227 K. Y. Goud, K. Mahato, H. Teymourian, K. Longardner, I. Litvan and J. Wang, *Sens. Actuators, B*, 2022, **354**, 131234.
228 R. K. Mishra, K. Y. Goud, Z. Li, C. Moonla, M. A. Mohamed, F. Tehrani, H. Teymourian and J. Wang, *J. Am. Chem. Soc.*, 2020, **142**, 5991–5995.

229 Y. Wu, F. Tehrani, H. Teymourian, J. Mack, A. Shaver, M. Reynoso, J. Kavner, N. Huang, A. Furmidge, A. Duvvuri, Y. Nie, L. M. Laffel, F. J. Doyle, M.-E. Patti, E. Dassau, J. Wang and N. Arroyo-Currás, *Anal. Chem.*, 2022, **94**, 8335–8345.
230 J. Xiao, C. Fan, T. Xu, L. Su and X. Zhang, *Sens. Actuators, B*, 2022, **359**, 131586.
231 S. Shajari, R. Salahandish, A. Zare, M. Hassani, S. Moossavi, E. Munro, R. Rashid, D. Rosenegger, J. S. Bains and A. Sanati Nezhad, *Adv. Sci.*, 2023, **10**, e2204171.
232 F. Ribet, A. Bendes, C. Fredolini, M. Dobielewski, M. Böttcher, O. Beck, J. M. Schwenk, G. Stemme and N. Roxhed, *Adv. Healthcare Mater.*, 2023, **12**, e2202564.
233 Z. Xue, L. Wu, J. Yuan, G. Xu and Y. Wu, *Biosensors*, 2023, **13**(2), 236.
234 Y. Song, J. Min, Y. Yu, H. Wang, Y. Yang, H. Zhang and W. Gao, *Sci. Adv.*, 2020, **6**(40), eaay9842.
235 S. S. Arya, S. B. Dias, H. F. Jelinek, L. J. Hadjileontiadis and A.-M. Pappa, *Biosens. Bioelectron.*, 2023, **235**, 115387.